Hindawi Publishing Corporation
Mathematical Problems in Engineering
Volume 2014, Article ID 324750, 25 pages
http://dx.doi.org/10.1155/2014/324750

Research Article

Automatic Extraction System for Common Artifacts in EEG Signals Based on Evolutionary Stone's BSS Algorithm

Ahmed Kareem Abdullah,[1,2] Chao Zhu Zhang,[1] Ali Abdul Abbas Abdullah,[2] and Siyao Lian[1]

[1] *College of Information and Communication Engineering, Harbin Engineering University, Harbin, Heilongjiang 150001, China*
[2] *Ministry of Higher Education and Scientific Research, Foundation of Technical Education, AL-Musaib Technical College, Babil 51006, Iraq*

Correspondence should be addressed to Ahmed Kareem Abdullah; ahmed_albakri1977@yahoo.com

Received 3 March 2014; Revised 17 June 2014; Accepted 17 June 2014; Published 18 August 2014

Academic Editor: Yingwei Zhang

An automatic artifact extraction system is proposed based on a hybridization of Stone's BSS and genetic algorithm. This hybridization is called evolutionary Stone's BSS algorithm (ESBSS). Original Stone's BSS used short- and long-term half-life parameters as constant values, and the changes in these parameters will be affecting directly the separated signals; also there is no way to determine the best parameters. The genetic algorithm is a suitable technique to overcome this problem by finding randomly the optimum half-life parameters in Stone's BSS. The proposed system is used to extract automatically the common artifacts such as ocular and heart beat artifacts from EEG mixtures without prejudice to the data; also there is no notch filter used in the proposed system in order not to lose any useful information.

1. Introduction

Electrical activities of the brain are usually measured by electroencephalogram (EEG) to describe the state of the patient's brain. The visual analysis for EEG activities by the technicians is very difficult because these activities are submerged with artifacts [1]. The artifacts are one of the limitations in the EEG acquisition unit and maybe taken mistakenly as wanted data in brain signal analysis or in a brain computer interface (BCI) system [2].

The common artifacts in EEG signals are power line noise interference (LN), electrocardiogram (ECG), and electrooculogram (EOG) [3]. Numerous approaches have been sophisticated in time, frequency, and time-frequency domains to remove or separate these artifacts [4].

Many researchers have been used blind source separation (BSS) techniques to separate the artifacts from brain signals [5]. Automatic removal approach of EOG artifacts from EEG data based on BSS is offered in [6]. Two ICA algorithms, InfoMax (IICA) and Extended-InfoMax (EIICA), were utilized to extract eye movements and power noise of 50 Hz from EEG data is proposed in [7]; the EIICA can isolate both super-Gaussian artifacts (eye blinks) and sub-Gaussian signal (power line noise interference), but IICA is only restricted to remove super-Gaussian artifacts (eye blinks). BSS and parallel factor analysis (PFA) are integrated to reject the EEG artifacts [8, 9]. Wavelet transforms (WT) with independent component analysis (ICA) and statistical autoregressive moving average model have been used to reject the artifacts [10]. Pesin [11] demonstrates a novel approach to recognize and reject eye blink artifacts from EEG system based on an integration between wavelet technique and FastICA to expose the temporal position of eye blink and then remove it. In recent years, new studies are used to extract the EEG data from EEG mixture based on modified BSS algorithms, such as in [2] which tries to propose a complete artifact rejection system based on constrained independent component analysis (cICA) to separate ECG and EOG artifacts from EEG signals measured inside MRI.

ICA algorithms usually used in EEG signal processing and the most widely used are Infomax [12], FastICA [13], SOBI [14], and BGSEP [15]; the SOBI and BGSEP used

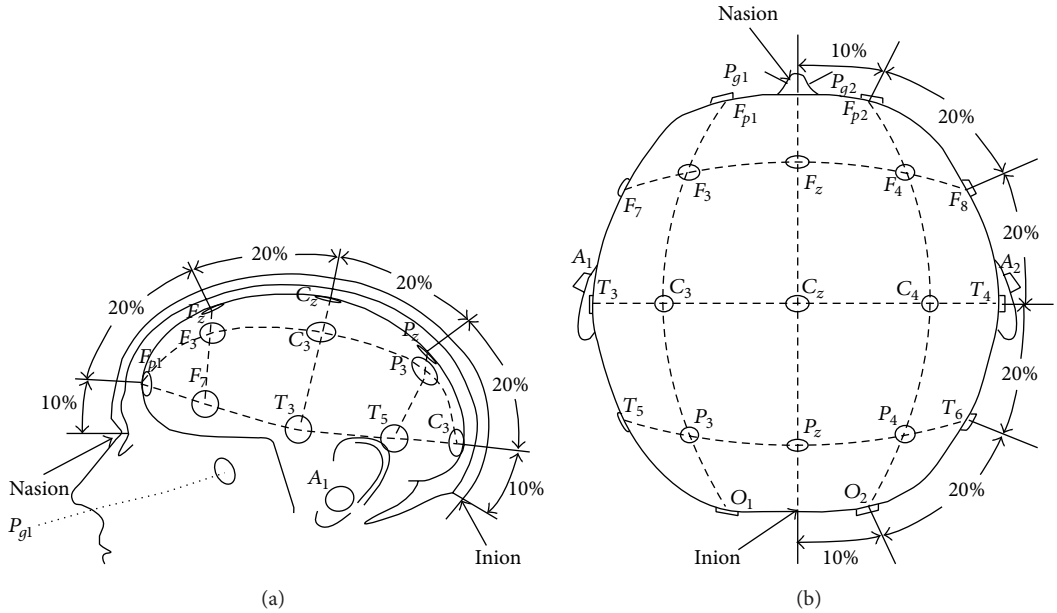

Figure 1: Electrodes placement over scalp based on 10–20 international EEG electrode system: (a) side view; (b) top view.

second-order statistic but the InfoMax and FastICA used high-order statistic [1]. A comparison study between ICA algorithms was proposed in [16]. ICA algorithms have an inherent disadvantage such as (i) source ambiguity, (ii) undetermined variances of the components, and (iii) the performance of ICA being decreased when the dataset is small and with large dataset the redundancy case is not sufficient to recover the independent components [2].

Stone's BSS is used instead of ICA due to these limitations [17–19]; it was first motivated by Stone [20]. Many researchers try to discuss and modify it to enhance the separation process [17, 21–23]. Stone's BSS was used successfully to extract the ocular artifact from EEG mixture [19].

Stone's BSS algorithm based on a temporal predictability measure to recover the sources from the mixture. Short- and long-term half-life parameters are used to calculate the temporal predictability of the signal; these parameters are taken as follows: *the long-term half-life is 100 times longer than corresponding short-term half-life*. The changes in these parameters will be affecting the output; also there is no technique to calculate the best values.

Evolutionary algorithms such as genetic algorithm (GA) and particle swarm optimization (PSO) are partly successful used to solve BSS problem in some applications but there are two issues addressed when using evolutionary algorithms to solve the BSS problem: (i) generating random initial coefficients of separate matrix W maybe does not give the candidate solutions; (ii) it is relatively slow due to large population size.

Due to the limitations in both original Stone's BSS and the genetic algorithm, the proposed algorithm is used to overcome these limitations by a hybridization technique of Stone's BSS with genetic algorithm.

Table 1: EEG frequency bands with brain state.

Name	Freq.	State of brain
Delta	<4 Hz	Sleeping/unconscious
Theta	4–8 Hz	Imagination
Alpha	8–13 Hz	Calm consciousness
Beta	13–35 Hz	Focused consciousness
Gamma	>35 Hz	Peak performance

Simple ad hoc criterion called sparsity measure proposed in [1] is used in the proposed system to classify the extracted signal into artifact or not. This criterion imposes the high amplitude and short duration artifact such as EOG and ECG.

In this paper, automatic artifact extraction system is proposed to clean the brain mixtures from common artifacts. This topic is identified as being of importance to the workers in brain signal analysis.

2. EEG Signals and Artifacts

The EEG system measures the brain signals by electrodes placed on the head surface (scalp); these electrodes (channels) are commonly arranged based on 10–20 international system as shown in Figure 1 [24]. This system has been incorporated by the American Electroencephalographic Society. In this system there are two reference points: nasion and inion to define the electrode location. The channel name indicates a specific brain regions, (F_p) frontal polar, (F) frontal, (C) central region, (P) parietal, (P_g) nasopharyngeal, (O) occipital area, and (A) ear lobe [24, 25]. The neurophysiological signals measured by EEG have different variation in amplitude, frequency, and shapes [26]. The frequency of EEG signal can be divided into 5 subbands as shown in Table 1 [11, 24, 27].

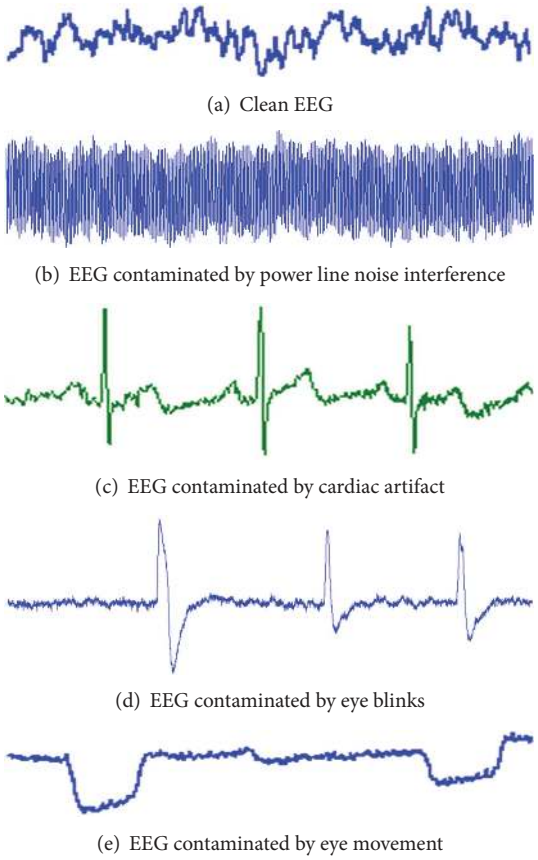

(a) Clean EEG

(b) EEG contaminated by power line noise interference

(c) EEG contaminated by cardiac artifact

(d) EEG contaminated by eye blinks

(e) EEG contaminated by eye movement

Figure 2: Common EEG artifacts waveforms.

EEG signal is highly nonstationary random weak signal (Figure 2(a)). The amplitude of EEG brain signals is divided into three divisions as shown in

$$\text{Amplitude} = \begin{cases} \text{Low} & < 20\,\mu\text{V} \\ \text{Medium} & 20\,\mu\text{V to } 50\,\mu\text{V} \\ \text{High} & \geq 50\,\mu\text{V}. \end{cases} \quad (1)$$

The artifacts represent one of the limitations in brain signal analysis and may be taken mistakenly as a brain signal. The common artifacts in EEG signal analysis are.

2.1. Power Line Noise Interference. Brain EEG signals are often contaminated by power line noise interference signal (50 or 60 Hz/AC power supply). This signal is monomorphic waveform and distributed in several electrodes. The power line noise signal is generated from wires, light fluorescents, and other tools in recording system. Usually the torch fluorescents' light produces an artificial spike in recorded signals from brain. Figure 2(b) shows the EEG signal submerged with power line noise waveform [3, 28].

2.2. Electrocardiography (ECG). The cardiac activity is a high electrical energy explicit effect on EEG signals. The ECG artifact is appear like regular spikes in EEG recording process as shown in Figure 2(c). These types of artifacts may be clinically misleading [29]. ECG artifact or heartbeat artifacts

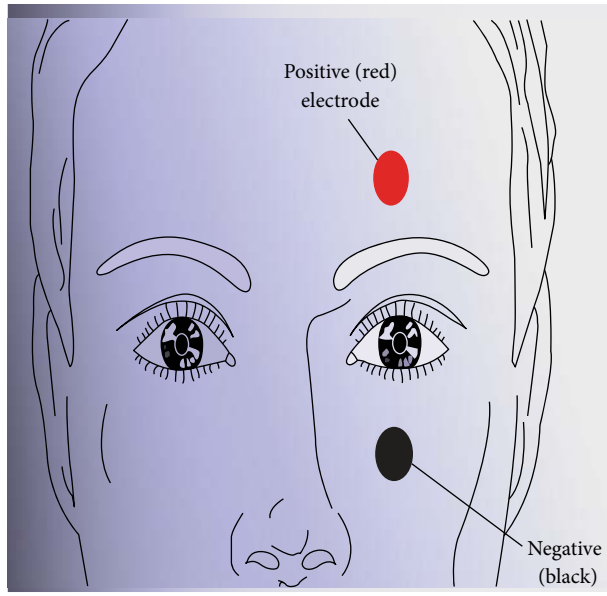

Figure 3: Place of EOG electrodes over single eye.

are produced when an electrode is placed on or near a blood vessel [27, 30].

2.3. Electrooculogram (EOG). The electrical activity produced by eye blinks or eye movement is known as the electrooculogram (EOG) artifact or ocular artifact (OA). The electrical dipole is generated by positive cornea and negative retina in the eye and the movements or blinks of human eye will be changing this dipole to produce EOG artifacts [19, 31]. Eye blink has spikes shape (Figure 2(d)) while the eye movements have square shapes (Figure 2(e)). The frequency of eye blink artifact is lower than 4 Hz. The eye blinks have low propagation but the eye movements have high propagation [32]. In the clinical interpretation these artifacts should be removed from EEG data. The EOG signal is measured by EOG electrodes placed above and under eye as shown in Figure 3 [30].

3. Artifact Rejection Methods

During the recording process the data are contaminated by different types of artifacts. These artifacts should be removed before analyzing the EEG signal. There are many techniques used for this purpose.

3.1. Manual Method. This is very simple method to eliminate the artifacts from EEG mixtures. The model for this method is governed by this condition:

if *artifact exists in epoch*, then *remove corrupted epoch*.

The important data will be lost during the removing process, particularly when limited amount of data are available or many artifacts submerged in EEG signals [33].

3.2. Filtering Method. This method depends on the analysis of frequency characteristic of EEG signal and artifacts. The frequency features provide efficient information for identifying the artifacts, but the spectra of artifacts are overlapped with EEG signal spectra. Therefore, the important data may be lost during the filtering process [34].

3.3. Regression Method. The regression method is based on the subtraction process for removing the artifact from contaminated EEG. The procedure for regression analysis to remove the ocular artifact is defined in [31]. The recorded EEG signal (EEG_r) can be described as the sum of original EEG signal (EEG_O) and a fraction (γ) of the EOG signal [31, 35]:

$$\mathrm{EEG}_r(k) = \mathrm{EEG}_O(k) + \gamma \mathrm{EOG}(k), \quad k = 1, 2, \ldots, M. \tag{2}$$

The correlation (R) at zero lag between EOG signal and observed EEG is given by

$$R = \sum_{K=1}^{M} \mathrm{EEG}_r(k)\,\mathrm{EOG}(k). \tag{3}$$

Substitute (2) in (3):

$$R = \sum_{K=1}^{M} \mathrm{EEG}_O(k)\,\mathrm{EOG}(k) + \gamma \sum_{K=1}^{M} \mathrm{EOG}(k)\,\mathrm{EOG}(k). \tag{4}$$

Equating (3) and (4) provides

$$\sum_{K=1}^{M} \mathrm{EEG}_r(k)\,\mathrm{EOG}(k) = \sum_{K=1}^{M} \mathrm{EEG}_O(k)\,\mathrm{EOG}(k) + \gamma \sum_{K=1}^{M} \mathrm{EOG}(k)^2. \tag{5}$$

However, in the regression technique, it is assumed that there is no correlation between the EEG_O and EOG; therefore,

$$\sum_{K=1}^{M} \mathrm{EEG}_O(k)\,\mathrm{EOG}(k) = 0. \tag{6}$$

Substitute (6) in (5):

$$\sum_{K=1}^{M} \mathrm{EEG}_r(k)\,\mathrm{EOG}(k) = \gamma \sum_{K=1}^{M} \mathrm{EOG}(k)^2. \tag{7}$$

From (7) the value of the propagation factor (γ) can be calculated by

$$\gamma = \frac{\sum_{K=1}^{M} \mathrm{EEG}_r(k)\,\mathrm{EOG}(k)}{\sum_{K=1}^{M} \mathrm{EOG}(k)^2}. \tag{8}$$

The EEG_O signal can be calculated by inserting the propagation factor γ in (2):

$$\mathrm{EEG}_O(k) = \mathrm{EEG}_r(k) - \gamma \mathrm{EOG}(k), \quad k = 1, 2, \ldots, M. \tag{9}$$

The regression approach is very easy in implementation but some of assumptions should be satisfied [11, 33, 36].

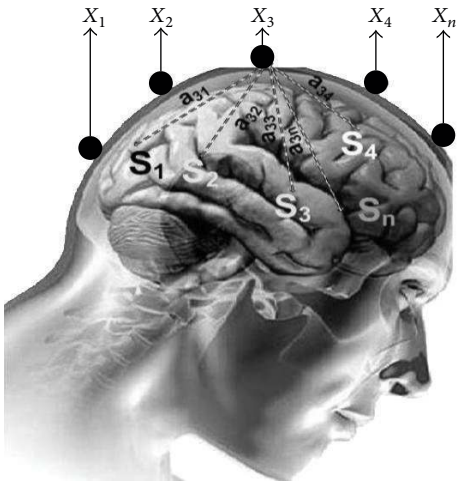

Figure 4: Brain signal analysis = BSS problem.

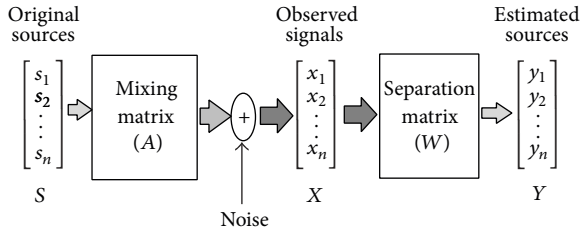

Figure 5: BSS schematic diagram.

(i) EEG signal and artifacts are uncorrelated.

(ii) The EEG signal is a linear combination.

(iii) The artifacts must not have any brain activity in order not to lose data at subtracting process.

(iv) Same propagation factors for different artifacts.

3.4. Blind Source Separation Method. In EEG acquisition unit, the electrodes are placed on the scalp at close distance and each electrode sensing a mixture of brain stimuli is based on the distance from the sources as shown in Figure 4 [2].

Many sources (neurons) are stimulated for any action in the brain and there is no information about the sources and the mixing procedure which happened inside the brain. Brain signal analysis is a blind source separation problem as mentioned in [2]. Typical BSS mixing model is shown in Figure 5 [18].

The mixing system without noise is

$$X(k) = AS(k), \tag{10}$$

where $X(k) = [x_1(k), \ldots, x_n(k)]^T$ are mixed signals from sensor (known), $S(k) = [s_1(k), \ldots, s_n(k)]^T$ are source signals (unknown), superscript T refers to transpose operator, $A \in R^{n \times n}$ is a mixing matrix (unknown), and the symbol k is time or sample index. The goal is to recover S from X without

Table 2: Limitations of artifact removing methods.

Method	Limitations
Manual	(i) Lose important data (ii) Difficult to control on eye blinks and maybe impossible to avoid it
Filtering	(i) Artifacts are overlapped with EEG (ii) Lose important data
Regression	(i) Difficult to obtain free reference (ii) Many assumptions must be satisfied
BSS	The separation is difficult or cannot if the amplitudes of the mixtures are comparable

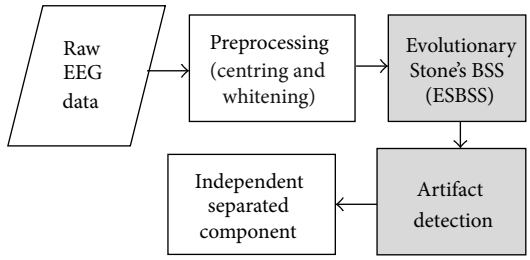

Figure 6: Schematic diagram of the automatic artifact extraction system.

knowing A; to solve this problem the separating matrix W should be founded to calculate the recovered signals by

$$Y(k) = WX(k), \tag{11}$$

where Y is a permutation of source signal S up to scaling factor.

Finally, the limitations summary for each method is shown in Table 2.

4. Proposed Work

Automatic artifact extraction system is proposed based on modified Stone's BSS (called evolutionary Stone's BSS algorithm (ESBSS)) and artifact detection measure to clean EEG-brain signals from common artifacts. ESBSS based on the joint between original Stone's BSS and genetic algorithms (GA). For easy reference, the outline of the proposed work is summarized in Figure 6.

Each block will be explained below.

(i) Raw EEG. Almost the brain electrical activities are measured by electroencephalography (EEG) device and the main characteristics of EEG signals are as follows: being easily recorded by electrodes, being complex-spatiotemporal signals, being very good in temporal regulation, being poor in spatial resolution, and depending on the number of electrodes [37]. These signals are submerged by artifact signals. Different raw EEG data are taken to test the proposed system as shown in the result section.

(ii) Preprocessing. The raw EEG data are preprocessed by centering and whitening techniques to make the BSS problem simple and better conditioned [38]. The centering process is very necessary to simplify the BSS estimation; it refers to centering the received variables by subtracting their sample mean (12); that is, remove the sample mean from received vectors and add it after recovering the original sources [27]:

$$x = \acute{x} - E[\acute{x}], \tag{12}$$

where x is the centered signal; $\acute{x}$ is the received signal; and $E[\acute{x}]$ is the expectation of $\acute{x}$.

The whitening process is a linear transformation used to simplify the calculation by transforming the received vector (X) to another vector $(\widetilde{X})$, whereby the whitened components are uncorrelated and their variance equals unity:

$$E\left[\widetilde{X}\widetilde{X}\right] = I. \tag{13}$$

Usually, the eigenvalue decomposition technique of the covariance matrix is used to obtain the whitening matrix:

$$C_x = E\left[\widetilde{X}\widetilde{X}^T\right] = EDE^T, \tag{14}$$

where C_x is the covariance matrix, E is the orthogonal matrix of eigenvector, and D is the diagonal matrix of eigenvalue.

The mixing matrix A is transformed to orthogonal mixing matrix $\widetilde{A}$:

$$\tilde{x} = ED^{-1/2}E^T x = ED^{-1/2}E^T AS = \widetilde{A}S, \tag{15}$$

where

$$\widetilde{A} = D^{-1/2}E^T AS. \tag{16}$$

The calculation of estimate n^2 parameters in A is reduced to $n(n-1)/2$ parameters in $\widetilde{A}$ [39].

(iii) Evolutionary Stone's BSS Algorithm (ESBSS). Evolutionary Stone's BSS algorithm is a joint between original Stone's BSS and genetic algorithm. The half-life parameters (h_{short}, h_{long}) values are generated randomly and tuned by genetic algorithm to enhance the separation process in original Stone's BSS.

Stone's BSS is based on the temporal predictability measure (TP) to separate the original sources from their mixture and its conjecture. The conjecture of Stone is as follows: *the TP of any signal mixture is* $\leq$ *that of any of its components*. This conjecture is used to find the weight vector which gives an orthogonal projection of mixtures [20]. Stone's measure of temporal predictability of signal $y(k)$ is defined as [20]

$$\begin{aligned} F(y) &= \log\frac{V_y}{U_y} = \log\frac{\sum_{k=1}^{N}\left(y_{\text{long}}(k) - y(k)\right)^2}{\sum_{k=1}^{N}\left(y_{\text{short}}(k) - y(k)\right)^2}, \\ y_{\text{short}}(k) &= \beta_S y_{\text{short}}(k-1) + \left(1-\beta_S\right)y(k-1), \\ y_{\text{long}}(k) &= \beta_L y_{\text{long}}(k-1) + \left(1-\beta_L\right)y(k-1), \end{aligned} \tag{17}$$

where N is the number of samples of $y(k)$, $\beta_s = 2^{-1/h_{\text{short}}}$, $\beta_L = 2^{-1/h_{\text{Long}}}$, and h_{short}, h_{long} are half-life parameters. The half-life h_{long} of β_L is 100 times longer than corresponding half-life h_{short} of β_S according to Stone [20], but this limitation

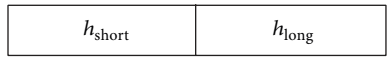

Figure 7: The chromosome representation.

maybe does not give the optimal solution; therefore the proposed work used genetic algorithm to find the optimum parameters which satisfied the better separation between the components.

GA is used to generate randomly half-life parameters (h_{long}, h_{short}) and tune these values until stopping criteria are satisfied instead of fixed values in original Stone's measure. Each chromosome consists of two real genes, where the first gene represents short-term half-life parameter h_{short} and the second gene represents long-term half parameter h_{long} as shown in Figure 7.

The parameters of the genetic algorithm are

(i) maximum number of generations = 20,

(ii) population size (pop.) = 40,

(iii) length of chromosome = 2,

(iv) probability of crossover = 0.95,

(v) probability of mutation = 0.05,

(vi) fitness function:

$$\text{Fit}(y) = \frac{1}{I(y) + \varepsilon} = \frac{1}{\sum_{i=1}^{n} H(y_i) - H(y_1, y_2, \ldots, y_n)}, \tag{18}$$

where $y_1, \ldots, y_n$ are separated signals, H is the entropy of the signals, $I(y)$ represent the mutual information calculated using the concept of differential entropy between n signals, and ε is a constant value (0.0001).

The mutual information is always nonnegative and zero if the components $(y_1, \ldots, y_n)$ are statistically independent. The epsilon (ε) constant is added to $I(y)$ in the denominator of the fitness function to avoid the infinity case. The definition of the fitness function parameter (Fit) is the key point in the performance of genetic algorithm [40].

GA attempts to maximize the fitness function by minimizing the mutual information $I(y)$ between the components and is significantly successful at this task. Therefore the inverse of the mutual information will be taken as a fitness function (18). The dependence among the separated components is minimized when the fitness is maximized [41].

For easy reference, the flowchart of the ESBSS is depicted in Figure 8.

The separated signals are calculated by $y(k) = w_i^T x(k)$, $W = [w_1, w_2, \ldots, w_n]$; then (17) is rewritten as

$$F(y_i) = \log \frac{w_i C_{xx}^{\text{long}} w_i^T}{w_i C_{xx}^{\text{short}} w_i^T}, \tag{19}$$

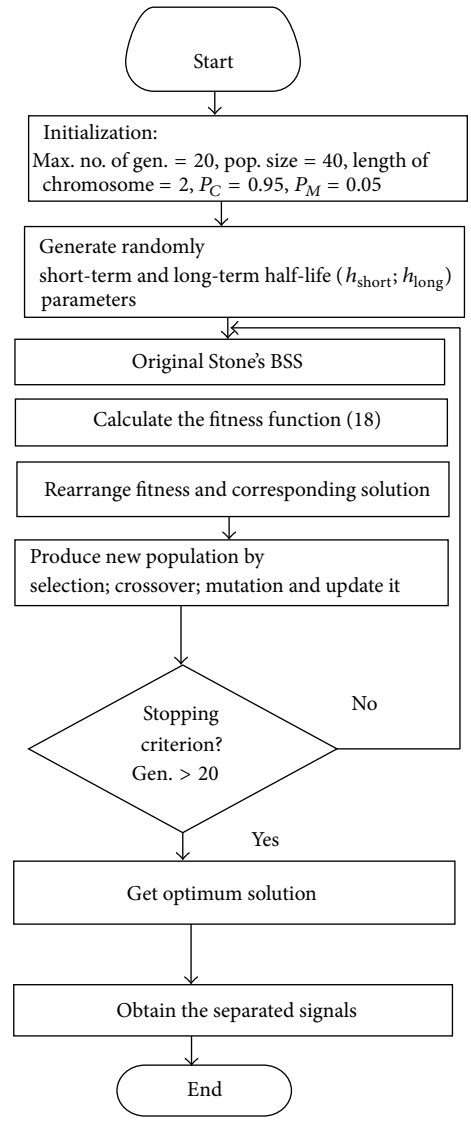

Figure 8: Evolutionary Stone's BSS Algorithm.

where C_{xx}^{long} is a long-term covariance matrix ($N \times N$) between signal mixtures; C_{xx}^{short} is a short-term covariance matrix ($N \times N$) between signal mixtures; $C_{x_i x_j}^{\text{long}}$ and $C_{x_i x_j}^{\text{short}}$ between ith and jth mixtures:

$$C_{x_i x_j}^{\text{short}} = \sum_{\tau} \left(x_{i\tau} - x_{i\tau}^{\text{short}}\right)\left(x_{j\tau} - x_{j\tau}^{\text{short}}\right),$$
$$C_{x_i x_j}^{\text{long}} = \sum_{\tau} \left(x_{i\tau} - x_{i\tau}^{\text{long}}\right)\left(x_{j\tau} - x_{j\tau}^{\text{long}}\right). \tag{20}$$

The main aim is to maximize Rayleigh's quotient ($F(y_i)$) to yield unmixing vectors; thereby generalized eigenvectors of $C_{xx}^{\text{long}}\,[C_{xx}^{\text{short}}]^{-1}$ are considered to solve this problem [20, 21, 42]; to find the eigenvectors $(W_1, W_2, W_3, \ldots, W_N)$ of

matrix ($C^{\text{short}^{-1}}C^{\text{long}}$) which are orthogonal in the covariance matrices,

$$W_i C^{\text{short}} W_j^t = 0, \quad W_i C^{\text{long}} W_j^t = 0, \tag{21}$$

where

$$W_i C^{\text{short}} W_j^t = \sum_\tau \left(y_{i\tau} - y_{i\tau}^{\text{short}}\right)\left(y_{j\tau} - y_{j\tau}^{\text{short}}\right), \quad W_i C^{\text{long}} W_j^t = \sum_\tau \left(y_{i\tau} - y_{i\tau}^{\text{long}}\right)\left(y_{j\tau} - y_{j\tau}^{\text{long}}\right). \tag{22}$$

When short-term half-life parameter h_{short} is toward zero value ($h_{\text{short}} \to 0$):

$$y_\tau^{\text{short}} \approx y_{\tau-1}, \quad \left(y_\tau - y_\tau^{\text{short}}\right) \approx \frac{d_{y_\tau}}{d\tau} = \acute{y}_\tau. \tag{23}$$

Also when long-term half-life parameter h_{long} is toward infinity ($h_{\text{long}} \to \infty$) and y has zero mean, the long-term mean is

$$y^{\text{long}} \approx 0, \quad \left(y_\tau - y_\tau^{\text{long}}\right) \approx y_\tau. \tag{24}$$

Now under these conditions the expectation for y_i and y_j is equal to zero:

$$E\left[y_i y_j\right] = 0. \tag{25}$$

Therefore, this indicates that each recovered signal y_i which can be calculated by $y_i = W_i x$ is uncorrelated with every other signal y_j which is also calculated by $y_j = W_j x$; also if y_i and y_j are independent, then the expectation value is also zero. This method is powerful for any linear mixture with statistically independent signals and is guaranteed to separate the independent components. Also the temporal derivative of each recovered signal is uncorrelated with every one and the expectation value equals zero:

$$E\left[\acute{y}_i \acute{y}_j\right] = 0. \tag{26}$$

The separating matrix W is calculated by Matlab eigenvalue function as

$$W = \text{eig}\left(C^{\text{long}} C^{\text{short}}\right). \tag{27}$$

One of the advantages of Stone's BSS is to simplify the BSS problem into generalized eigenproblem [22].

(i) *Artifact Detection.* The artifact detection process is based on simple ad hoc criterion called sparsity measure (28) which is implemented by [1].

(ii) Consider

$$\text{Sparsity}\left(y^{(j)}\right) = \frac{\max\left[\left|y_i^{(j)}\right|\right]}{\text{std}\left[y_i^{(j)}\right]} \log\left(\frac{\text{std}\left[y_i^{(j)}\right]}{\text{median}\left[\left|y_i^{(j)}\right|\right]}\right), \tag{28}$$

where $y^{(j)} = [y_1^{(j)}, \ldots, y_N^{(j)}]$ is the jth components, N is the number of samples in the frame, std is the standard deviation, and i is the time index.

This criterion imposes that the artifacts with high amplitude have short duration compared with selected frame length; this is called sparse in a time domain [1]. The sparsity value equals 2.5 for super-Gaussian artifact (i.e., EOG and ECG) as mentioned in [1] but for sub-Gaussian signal (i.e., power line noise interference) it is less than 1 as concluded from the simulation and experimental results.

5. Results

Simulated and real EEG data are tested by the proposed system. The performance of the simulated and semisimulated data is evaluated by interference signal ratio ISR (29) and a cross-correlation measure between the original and estimated artifacts:

$$\text{ISR}_i = 10 \log \frac{E\left[\left(s_i(k) - y_i(k)\right)^2\right]}{E\left[\left(s_i(k)\right)^2\right]}, \tag{29}$$

where $s(k)$ is the original signals, $y(k)$ is the recovered signals, and k is the time or sample index.

The result of the separating process is better whenever the ISR measure is less. For real EEG data the ISR measure is not applicable because there is no information about the original sources. Therefore, EOG electrodes (vEOG and hEOG) are used to measure the face activity (artifacts) and then compare these artifacts with extracted artifacts. The results are compared with the different BSS algorithms (EFICA [43], original Stone's BSS [20], FICA, SOBI, and JADE). The power line noise interference 50 Hz is separated as a biological artifact; that is, there is no notch filter used during the recording process in order not to lose any useful information around 50 Hz, where the gamma band (25–100 Hz) lies within the notch filter range.

5.1. Simulation Results. Simulated EEG signal and common artifacts (LN, EOG, and ECG) are generated in Matlab program based on [2, 44, 45].

For easy reference, the procedure is divided into four steps.

Step 1 (generate artificial sources.) EEG signal is very weak compared with artifacts. It is highly nonstationary random signal and notable in the frequency domain characteristics. Almost the artifacts have high amplitude and are localized in the time and/or in frequency domains [46]. The simulation of EEG signal and different types of artifacts is implemented based on the characteristics of each signal. Predominantly

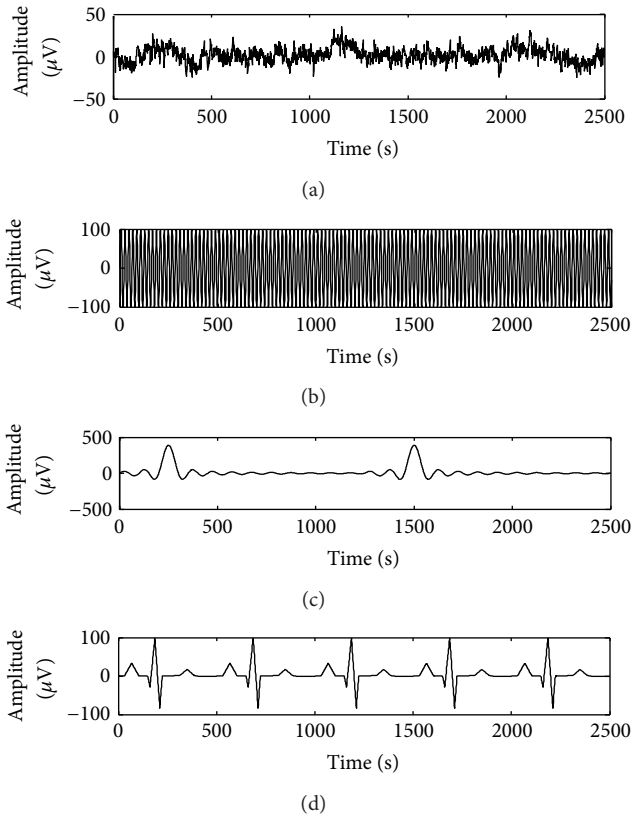

Figure 9: Artificial sources: (a) EEG, (b) line noise, (c) eye blink artifact, and (d) heartbeat artifact.

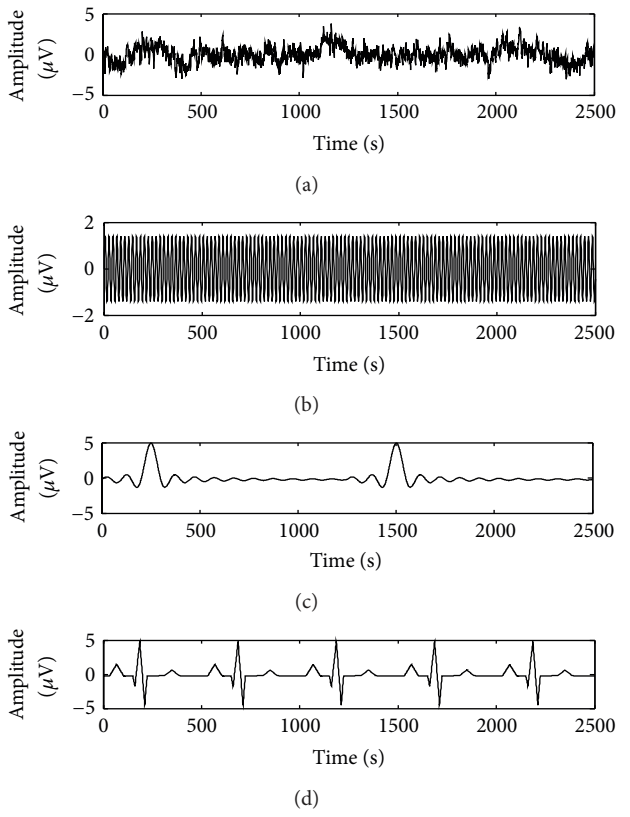

Figure 10: Artificial source with zero mean and unit variance.

two theories are widely used to generate simulated EEG signals: classical and phase-resetting theories [2, 44, 45]. In classical theory, the peaks in event-related potential (ERP) waveforms reflect phasic bursts of activity in one or more brain regions that are triggered by experimental events of interest. Specifically, it is assumed that an ERP-like waveform is evoked by each event, the ERP "signal" is buried in ongoing EEG signal "noise."

In the phase-resetting theory, the experimental events reset the phase of ongoing oscillations [44]. The phase-resetting method which is proposed in [44] is used here to generate the data. Figure 9 shows the simulated original artificial signals (S) for EEG and different types of artifacts EOG, ECG, and LN. Eye blink artifact is simulated using Sinc function [45, 47], ECG artifact is simulated using ecg function in Matlab, and the power line noise interference is simulated based on sinusoidal function (50 Hz). Figure 10 shows the signals with zero mean and unit variance.

Step 2 (mixing process). The signals are mixed randomly by mixing matrix A to produce mixture X. All the possibilities of the mixing process are taken as shown in the schematic diagram of the mixing (Figure 11) in order to cover all the expected mixtures and to produce different types of mixtures (Figures 12, 13, 14, 15, and 16).

Step 3 (extraction process.) The EEG signals considered a projection of a group of mixed signals from brain data and artifact. The main challenge in the human brain signal analysis is to clean the EEG data from common artifacts by separating the mixture into its individual components. ESBSS algorithm is used to extract the artifact signals from brain mixture. Very good extraction results are obtained by ESBSS as shown in Figures 17, 18, 19, 20, and 21. In these figures the extracted signals are shifted vertically for display purposes.

The comparison of ISR value for different BSS algorithms is shown in Tables 3, 4, 5, 6, and 7. ESBSS algorithm is surpassed significantly for other BSS algorithms as shown in Tables 8, 9, 10, 11, and 12.

Step 4 artifact Detection. Sparsity measure is used to detect the artifacts as mentioned in the proposed work section. Table 13 classifies the separated components based on sparsity value. For power line noise the sparsity value is very low (less than 1) but for EOG or ECG artifacts the sparsity value is high (more than 2.5) [1].

5.2. Semisimulated Data. Real EEG signals are apparently artifact-free signals recorded from a newborn individual with active sleep (Figures 22(a1) and 22(a2)). These signals are mixed randomly (Figure 23) with simulated artifacts to produce contaminated data (Figure 24). The real EEG data are available in http://sisec2010.wiki.irisa.fr/. Sinc function

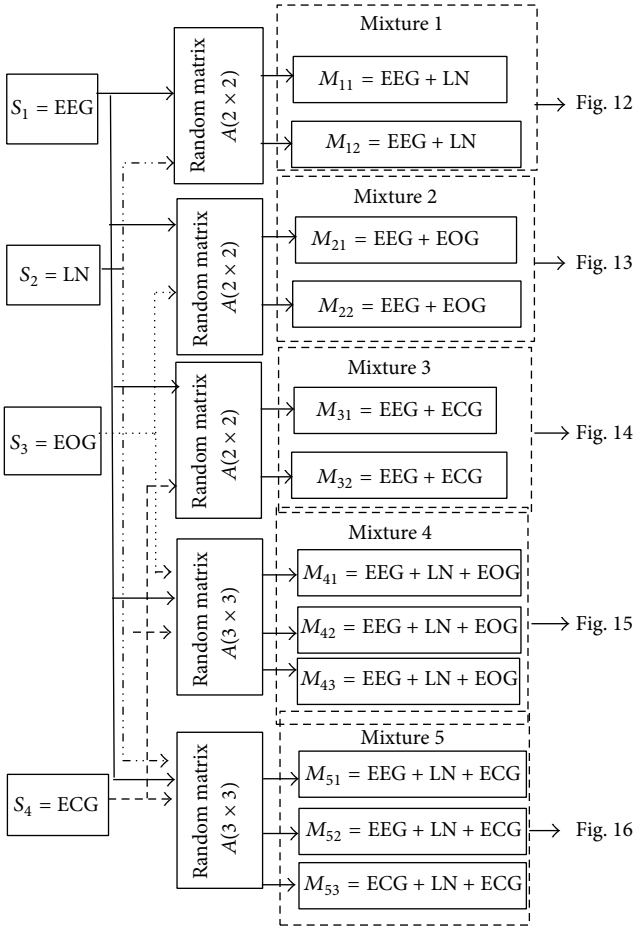

Figure 11: Schematic diagram of mixing process.

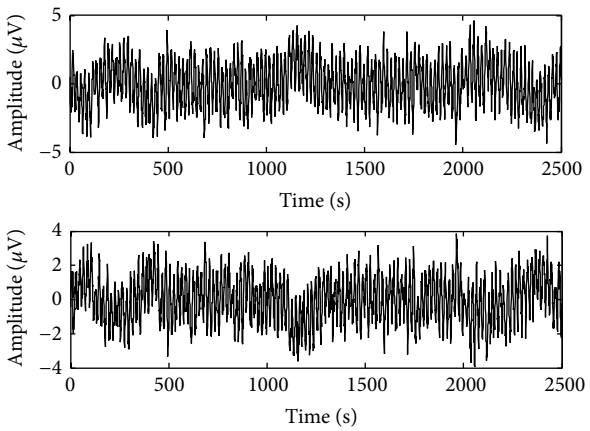

Figure 12: Mixture 1 (EEG + LN).

is used to produce the shape of eye blinking artifact [45]. Heartbeat artifact is simulated by ecg function in Matlab; the power line noise interference is simulated by sin function.

Figure 25 shows the original source signals and corresponding recorded signals using the ESBSS algorithm shifting vertically for display purposes.

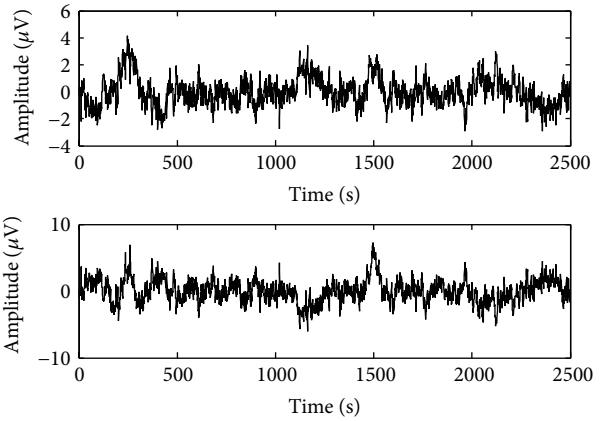

Figure 13: Mixture 2 (EEG + EOG).

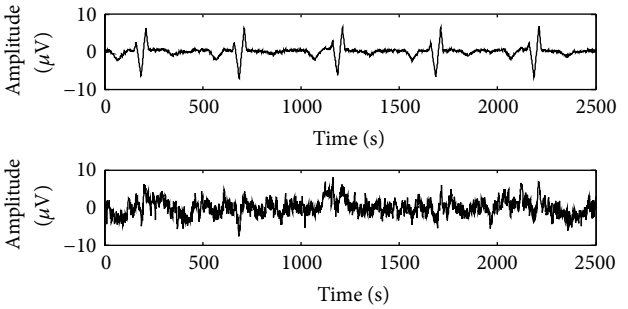

Figure 14: Mixture 3 (EEG + ECG).

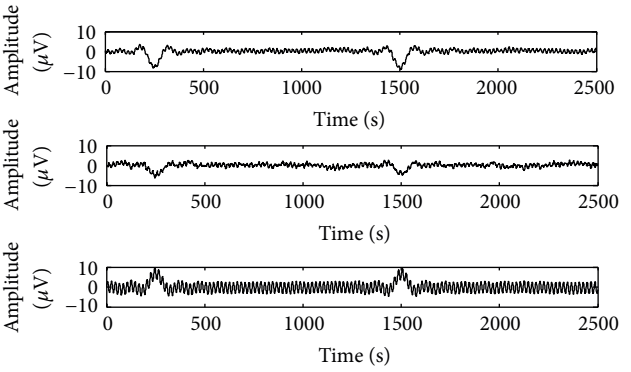

Figure 15: Mixture 4 (EEG + LN + EOG).

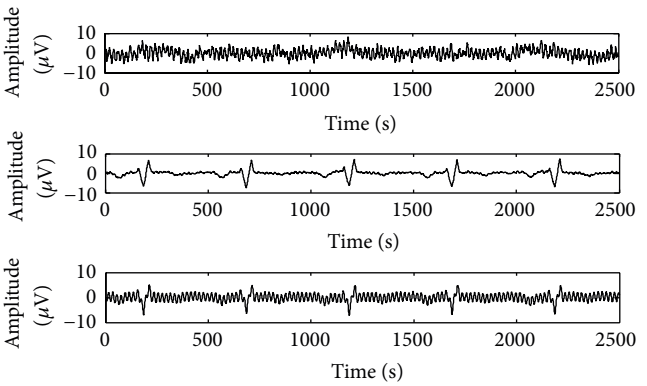

Figure 16: Mixture 5 (EEG + LN + ECG).

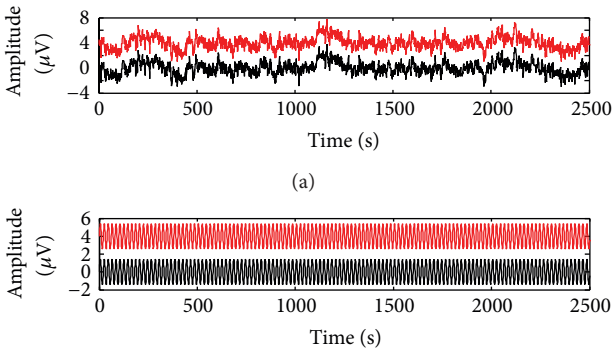

FIGURE 17: Source with its recovered signal using ESBSS shifted vertically for display purposes: (a) EEG signal; (b) LN.

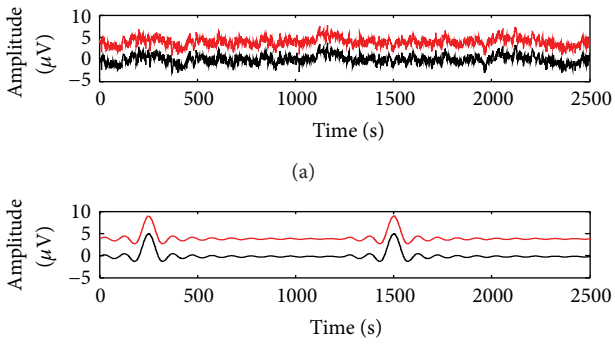

FIGURE 18: Source with its recovered signal using ESBSS shifted vertically for display purposes: (a) EEG signal; (b) EOG artifact.

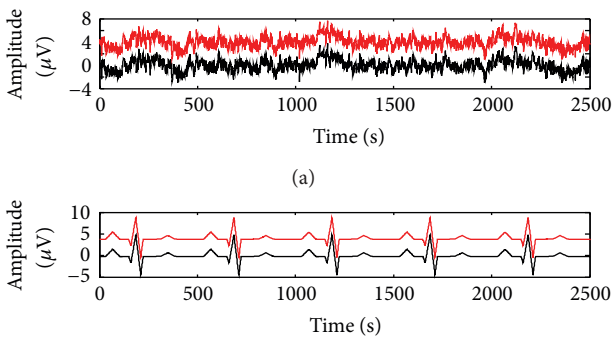

FIGURE 19: Source with its recovered signal using ESBSS shifted vertically for display purposes: (a) EEG signal; (b) ECG artifact.

The performance of the ESBSS algorithm is evaluated by interference to signal ratio ISR as shown in Table 14. Another performance evaluation measure based on cross-correlation between original and the estimated artifact is shown in Table 15.

The sparsity value is used to indicate the artifact components; for short-duration artifacts (i.e., eye blinking and heartbeat) the sparsity value should exceed 2.5 [1], but for line noise interference it should not exceed 1. Therefore, if the sparsity value for any separated component lies within this

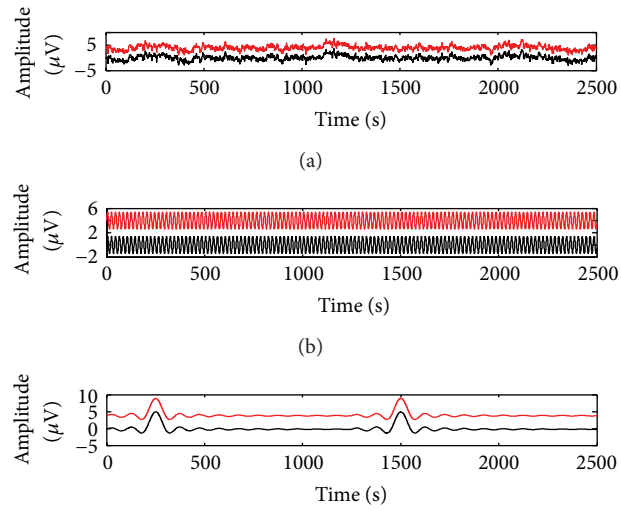

FIGURE 20: Source with its recovered signal using ESBSS shifted vertically for display purposes: (a) EEG signal; (b) LN; (c) EOG artifact.

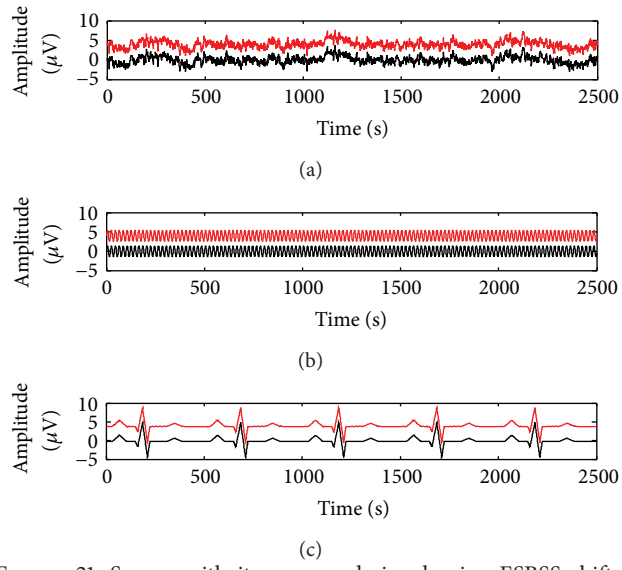

FIGURE 21: Source with its recovered signal using ESBSS shifted vertically for display purposes: (a) EEG signal; (b) LN; (c) ECG artifact.

limitation ($2.5 \leq \text{SP} \leq 1$), then the separated component is artifacts as shown in Table 16.

5.3. Real Data with 8 Channels. Real EEG data are taken from computerized EEG device. Two studies are implemented with the main goal being to extract the artifact as independent components. The brain signals are recorded from six electrodes (F_{p1}, F_{p2}, C_3, C_4, O_1, and O_2) placed on the scalp according to 10–20 system with a ground placed at C_z as shown in Figure 26; the sampling rate is 256 Hz. Furthermore, the EOG electrodes (vEOG and hEOG) are used to measure EOG activity from eyes; these electrodes are placed above and on the side of the left eye socket. The EOG channels (vEOG and hEOG) are used to assess the performance of the proposed system.

Table 3: ISR measure for separating Mixture 1.

BSS methods	ISR		ISR
	LN	EEG	mean
EBSS	−34.8361	−86.3115	−60.5738
EFICA	−35.2846	−60.5163	−47.9005
Stone	−34.0042	−52.2436	−43.1239
FICA	−33.8766	−55.8967	−44.8867
SOBI	−33.3401	−50.8478	−42.094
JADE	−33.3296	−50.7693	−42.0495

Table 4: ISR measure for separating Mixture 2.

BSS methods	ISR		ISR
	EOG	EEG	mean
EBSS	−28.9238	−74.2053	**−51.5646**
EFICA	−26.7285	−73.1821	−49.9553
Stone	−48.3132	−67.3195	−57.8164
FICA	−32.3676	−31.2014	−31.7845
SOBI	−30.7037	−29.4485	−30.0761
JADE	−30.7178	−29.4607	−30.0893

Table 5: ISR measure for separating Mixture 3.

BSS methods	ISR		ISR
	ECG	EEG	mean
EBSS	−19.3825	−47.0354	−33.209
EFICA	−19.1334	−45.2645	−32.199
Stone	−13.6593	−19.2579	−16.4586
FICA	−26.0624	−26.2457	−26.1541
SOBI	−29.4528	−23.7752	−26.614
JADE	−29.4542	−23.7745	−26.6144

Table 6: ISR measure for separating Mixture 4.

BSS methods		ISR		ISR
	LN	EOG	EEG	mean
EBSS	−27.9257	−66.5205	−72.5359	−55.6607
EFICA	−26.1559	−60.1094	−71.5945	−52.6199
Stone	−33.9812	−52.7812	−64.4604	−50.4076
FICA	−30.3523	−55.9096	−31.3082	−39.19
SOBI	−28.7800	−49.5674	−29.4057	−35.9177
JADE	−30.6898	−34.2503	−29.4202	−31.4534

Table 7: ISR measure for separating Mixture 5.

BSS methods		ISR		ISR
	LN	ECG	EEG	mean
EBSS	−19.2476	−74.9845	−31.2020	−41.8114
EFICA	−19.0203	−59.8420	−31.1511	−36.6711
Stone	−22.0368	−51.4257	−29.6362	−34.3662
FICA	−24.5847	−55.4876	−23.1855	−34.4193
SOBI	−27.6806	−17.7063	−18.3194	−21.2354
JADE	−28.9144	−17.9272	−18.5233	−21.7883

Table 8: Correlation measure (Mixture 1).

BSS methods	LN with: Mixture 1		Estimated sources	
	M_1	M_2	LN	EEG
EBSS	0.9579	0.9994	1.0000	0.0321
EFICA	0.9579	0.9994	1.0000	0.0319
Stone	0.9579	0.9994	1.0000	0.0324
FICA	0.9579	0.9994	1.0000	0.0324
SOBI	0.9579	0.9994	1.0000	0.0327
JADE	0.9579	0.9994	1.0000	0.0327

Table 9: Correlation measure (Mixture 2).

BSS methods	EOG with: Mixture 2		Estimated sources	
	M_1	M_2	EOG	EEG
EBSS	0.9579	0.9994	1.0000	0.0319
EFICA	0.9579	0.9994	1.0000	0.0321
Stone	0.9579	0.9994	1.0000	0.0324
FICA	0.9579	0.9994	1.0000	0.0324
SOBI	0.9579	0.9994	1.0000	0.0327
JADE	0.9579	0.9994	1.0000	0.0327

Table 10: Correlation measure (Mixture 3).

BSS methods	ECG with: Mixture 3		Estimated sources	
	M_1	M_2	ECG	EEG
EBSS	0.9579	0.9994	1.0000	0.0321
EFICA	0.9579	0.9994	1.0000	0.0319
Stone	0.9579	0.9994	1.0000	0.0324
FICA	0.9579	0.9994	1.0000	0.0324
SOBI	0.9579	0.9994	1.0000	0.0327
JADE	0.9579	0.9994	1.0000	0.0327

Table 11: Correlation measure (Mixture 4).

BSS methods	LN with: Mixture 4			estimated sources			EOG with: Mixture 4			Estimated sources		
	M_1	M_2	M_3	LN	EOG	EEG	M_1	M_2	M_3	LN	EOG	EEG
EBSS	0.1628	0.3007	0.8638	1.0000	0.0321	0.0093	0.8342	0.3167	0.3555	0.3339	1.0000	0.0092
EFICA	0.1628	0.3007	0.8638	1.0000	0.0319	0.0093	0.8342	0.3167	0.3555	0.3336	1.0000	0.0093
Stone	0.1628	0.3007	0.8638	1.0000	0.0323	0.0093	0.8342	0.3167	0.3555	0.0092	1.0000	0.3348
FICA	0.1628	0.3007	0.8638	1.0000	0.0097	0.0324	0.8342	0.3167	0.3555	0.9996	1.0000	0.0092
SOBI	0.1628	0.3007	0.8638	1.0000	0.0103	0.0327	0.8342	0.3167	0.3555	0.9994	1.0000	0.0093
JADE	0.1628	0.3007	0.8638	1.0000	0.0344	0.0103	0.8342	0.3167	0.3555	0.3341	1.0000	0.0107

The ISR index is not applicable for real EEG data because the mixing process is unknown. Therefore, the correlation measure is used to calculate the correlation between extracted artifacts and the recorded artifacts (i.e., EOG channels). The sparsity measure is used to classify the separated components signal into artifact or not [48].

5.3.1. Data Set I. The EEG signals are contaminated by eye blink artifact and power line noise 50 Hz. Eye blinking artifact is clearly in the frontal channels (F_{p1}, F_{p2}) and decreased in the distance of the electrodes from the eye. All the EEG channels are contaminated by power line noise 50 Hz but with strongly different contamination. Power line noise is

Table 12: Correlation measure (Mixture 5).

BSS methods	LN with: Mixture 5			estimated sources			ECG with: Mixture 5			Estimated sources		
	M_1	M_2	M_3	LN	ECG	EEG	M_1	M_2	M_3	LN	ECG	EEG
EBSS	0.7835	0.0980	0.8406	1.0000	0.0329	0.0203	0.6273	0.5379	0.3951	0.1200	1.0000	0.0365
EFICA	0.7835	0.0980	0.8406	1.0000	0.0328	0.0203	0.6273	0.5379	0.3951	0.1199	1.0000	0.0366
Stone	0.7835	0.0980	0.8406	1.0000	0.0574	0.0331	0.6273	0.5379	0.3951	0.1215	1.0000	0.0365
FICA	0.7835	0.0980	0.8406	1.0000	0.0329	0.0839	0.6273	0.5379	0.3951	0.1225	1.0000	0.0365
SOBI	0.7835	0.0980	0.8406	1.0000	0.1304	0.0331	0.6273	0.5379	0.3951	0.1233	1.0000	0.1232
JADE	0.7835	0.0980	0.8406	1.0000	0.0316	0.1270	0.6273	0.5379	0.3951	0.1235	1.0000	0.1202

Table 13: Types of separated signals from simulated mixtures of the proposed algorithm using sparsity measure.

Signals	Mixture 1		Mixture 2		Mixture 3		Mixture 4			Mixture 5		
	y_1	y_2	y_1	y_2	y_1	y_2	y_1	y_2	y_3	y_1	y_2	y_3
Sparsity value	0.2731	1.7983	10.5601	1.9832	11.9361	1.7809	0.5172	9.6739	2.1691	0.3871	8.6791	2.1479
Type of signal based on sparsity	LN	Brain signal	Artifact	Brain signal	Artifact	Brain signal	LN	Artifact	Brain signal	LN	Artifact	Brain signal

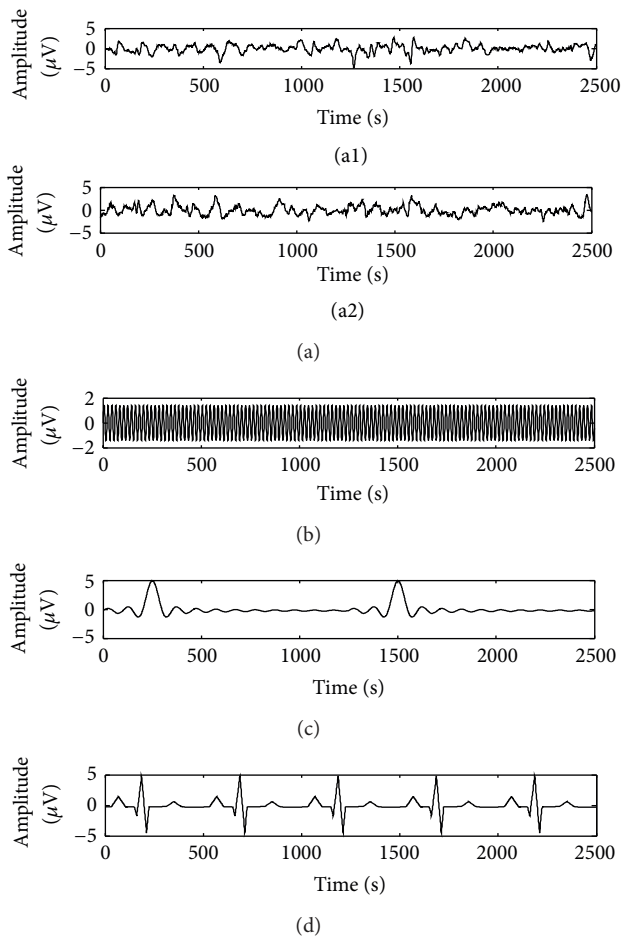

Figure 22: EEG and artifact signals.

pronounced on the central and occipital channels (i.e., C_3, C_4, O_1, and O_2) [48] as shown in Figure 27(a). By very good extraction of the line noise interference and eye blink artifact by the ESBSS algorithm, the line noise is concentrated

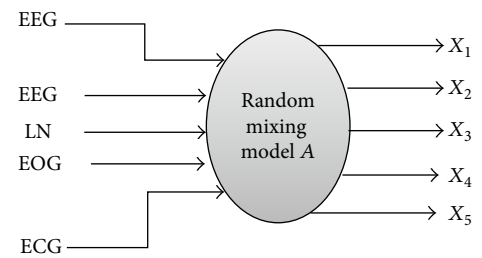

Figure 23: Schematic diagram of the mixing process.

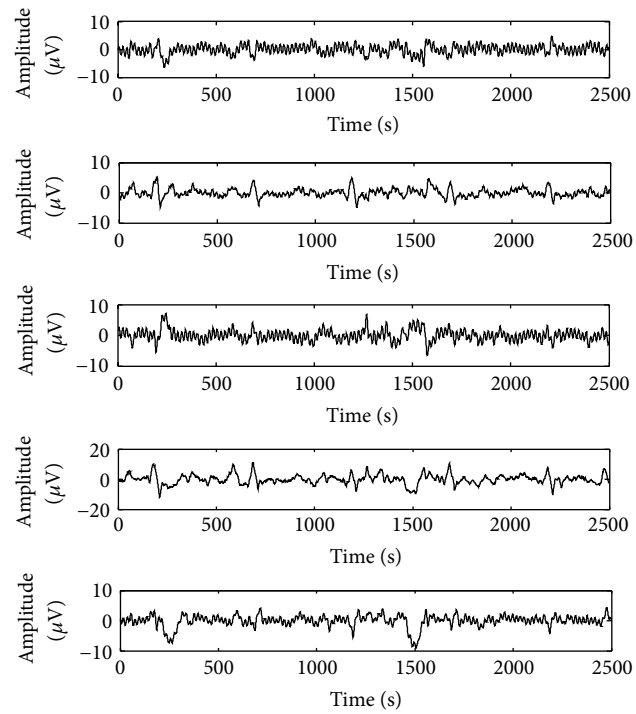

Figure 24: Contaminated signals (mixtures).

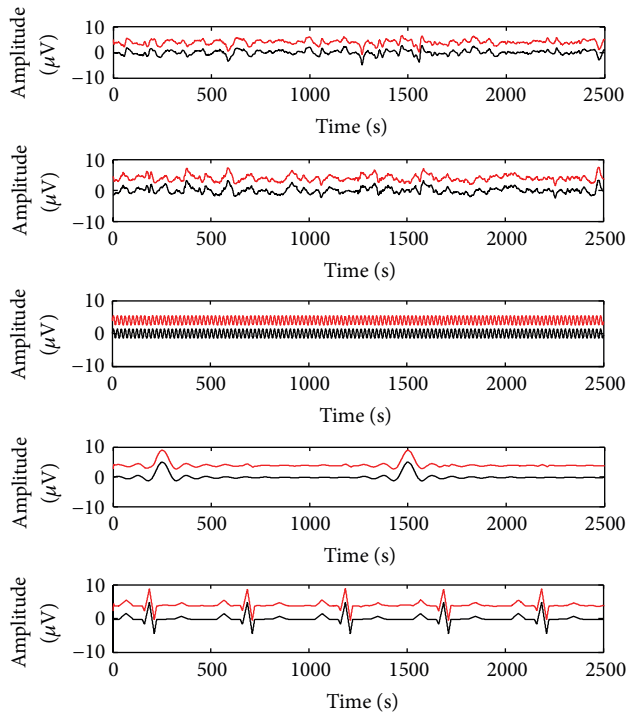

Figure 25: Recorded and corresponding recovered signals by EBSS shifted vertically for display purposes.

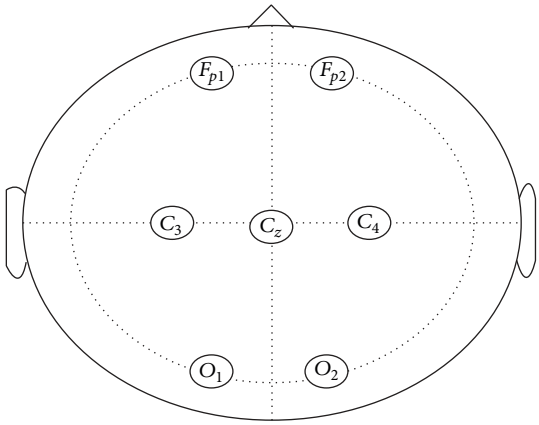

Figure 26: Placement of electrodes.

and separated in IC_1 (Figure 28) and the eye blink artifact is clearly isolated in IC_6 as shown in Figure 28. Table 17 shows the correlation between vEOG channel (Figure 27(b)) and extracted eye blink artifact component (IC_1) (Figure 28). The correlation result illustrates that the ESBSS algorithm is more powerful than other BSS algorithms to extract the eye blinking artifact. Table 18 shows type of separated components based on sparsity value, where IC_1 is a power line noise because its value is very low (less than 1), and the IC_6 is classified as the artifact signal due to high sparsity value (more than 2.5).

The result is also confirmed by power spectra of the mixture signals and extracted components. As mentioned above, all channels are interference with line noise 50 Hz, particularly O_1, O_2, C_3, and C_4 as shown in Figure 29. The frequency components of the extracted signals showed that the power line noise was successfully extracted by ESBSS as shown in Figure 30.

5.3.2. Data Set II. The EEG channels are contaminated by eye movement (eye muscle artifact) and eye blinking artifact as well as by power line noise interference during the recording process. Eye muscle artifacts present in all channels; eye blink artifacts appear strongly in the frontal channels and the power line noise 50 Hz strongly appears on the central and occipital channels as shown in Figure 31. Good extraction of the artifacts by EBSS algorithm is shown in Figure 32. The line noise is concentrated and separated in IC_1, and the eye muscle artifact is isolated in IC_5 and the eye blink artifact is clearly isolated in IC_6. The performance of the proposed system is tested by the correlation between EOG channels (Figure 31(b)) with the extracted artifacts as shown in Table 19. The sparsity value is used to indicate the artifact components as shown in Table 20. The frequency components of the EEG data and extracted components around 50 Hz range showed that the power line noise is successfully isolated as shown in Figures 33 and 34.

5.4. Real EEG with 19 Channels. Real EEG data contaminated by power line noise interference and EOG artifact (eye blink) are measured by computerized EEG device in Ibn-Rushd Hospital, Baghdad, Iraq. The computerized EEG is a computer with a PCI card of data acquisition unit that acquires the signals from the scalp through macroelectrodes as shown in Figure 35.

Table 14: Compression of ISR.

BSS methods	Interference signal ratio (ISR) for estimating signals (y_1, y_2, y_3, y_4, and y_5)					ISR mean
	y_1	y_2	y_3	y_4	y_5	
EBSS	−5.5877	−11.8889	−33.9764	−21.9881	−21.3926	−18.9667
EFICA	−4.9921	−9.9699	−28.9281	−21.9773	−18.8879	−16.9511
Stone	−4.1781	−10.3881	−33.8844	−13.1918	−21.1616	−16.5608
FICA	−4.5967	−9.6643	−16.427	−21.0723	−15.8339	−15.7494
SOBI	−3.9981	−13.891	−16.1158	−20.7612	−18.1621	−14.5856
JADE	−3.8818	−13.743	−16.7134	−20.8741	−17.8801	−14.6185

Table 15: Comparison of correlation measure.

BSS	Correlation between original and estimated artifact		
	Line noise $LN_{Estimated}$	Eye blink $EOG_{Estimated}$	Heartbeat $ECG_{Estimated}$
EBSS	0.9999	0.9980	0.9992
EFICA	0.9948	0.9971	0.9971
Stone	0.9998	0.9877	0.9962
FICA	0.9547	0.9961	0.9870
SOBI	0.9331	0.9851	0.9934
JADE	0.9893	0.9959	0.9927

Table 16: Types of separated signals from semi simulated mixtures of the proposed algorithm using sparsity measure.

Signals	Recovered signals				
	y_1	y_2	y_3	y_4	y_5
Sparsity value	1.9871	1.8872	0.3411	8.98321	12.9712
Type of signal based on sparsity	Brain signal	Brain signal	LN	Artifact	Artifact

One healthy subject, male, 24 years old, participated in this study. EEG signals were measured using 19 electrodes used to measure the brain signals placed on the scalp according to 10–20 system and referenced against forehead [27]. According to the specification of computerized EEG device the recorded signals were digitized at 256 Hz, and trail length is 10 Sec (10 sec × 256 Hz = 2560 sampls), during which the subject was allowed to perform eyes blink artifacts.

The block diagram of the proposed procedure is explained in Figure 36.

After the EEG trace has been finished, it can be saved as an ASCII code from

File > Export >.

This ASCII file can be opened using the Notepad program. Figure 37 shows the EEG trace arranged in columns (the sequences of channels are predefined). The data is imported into Microsoft Excel program to delete the first column that contains the timing information and to delete the channel's names as shown in Figure 38, and then the data is imported into Matlab.

Figure 39 shows the contaminated signals; these signals are preprocessed for simplification as shown in Figure 40. ESBSS and different BSS algorithms were applied to 19 channels of 10-second data to extract the power line noise 50 Hz and eye blink artifact. Figure 41 represents the extracted components by ESBSS algorithms. The eye blink artifact is separated successfully in IC_1 and the power line noise interference is separated in IC_7 without using notch filter. The performance of the proposed system is evaluated by the correlation measure between EOG channel and the estimated artifact as shown in Table 21. The separated signals are classified based on sparsity measure as shown in Table 22.

Table 17: Correlation measure between vEOG and eye blinking artifact for different types of BSS.

BSS	Correlation between vEOG and estimated eye blink artifact
EBSS	0.9997
EFICA	0.9981
Stone	0.9767
FICA	0.9554
SOBI	0.9555
JADE	0.9777

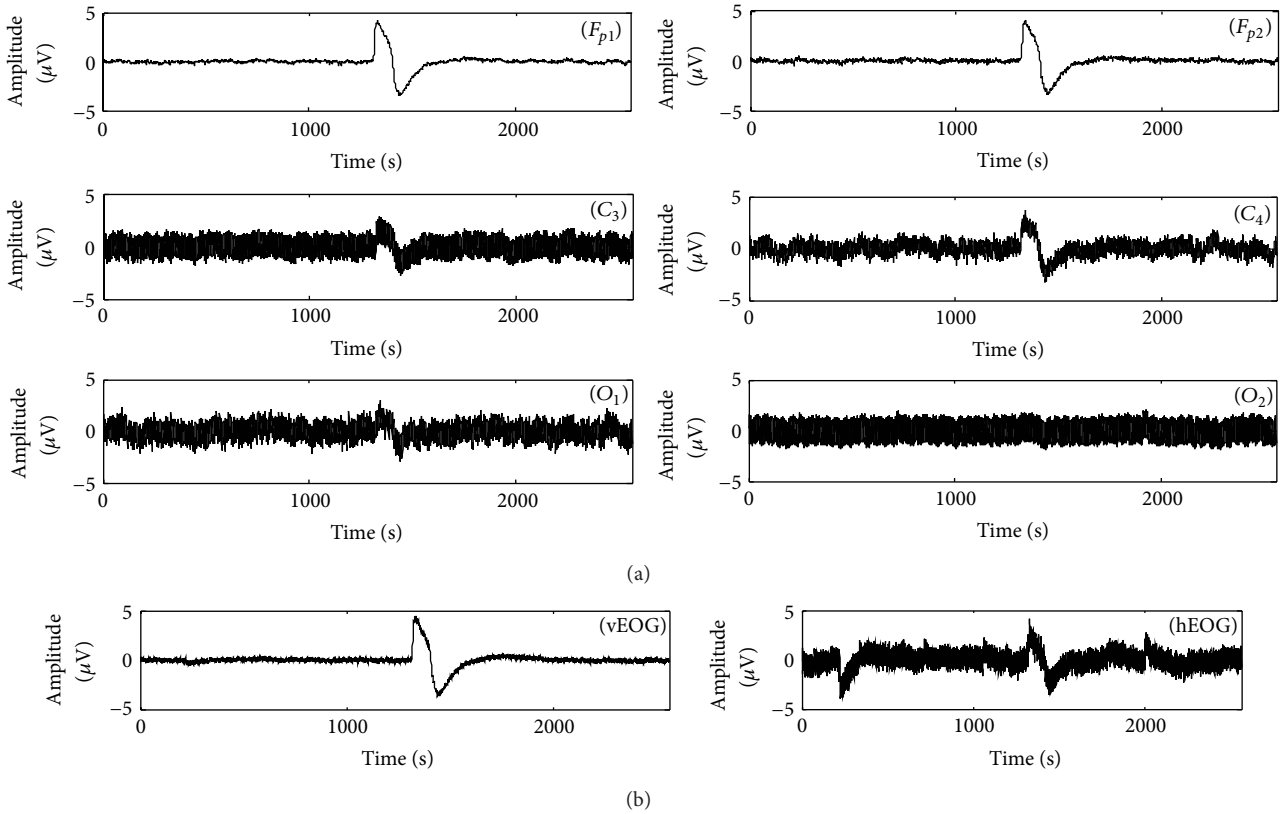

Figure 27: Data set I with zero mean and unit variance: (a) EEG electrodes; (b) EOG electrodes.

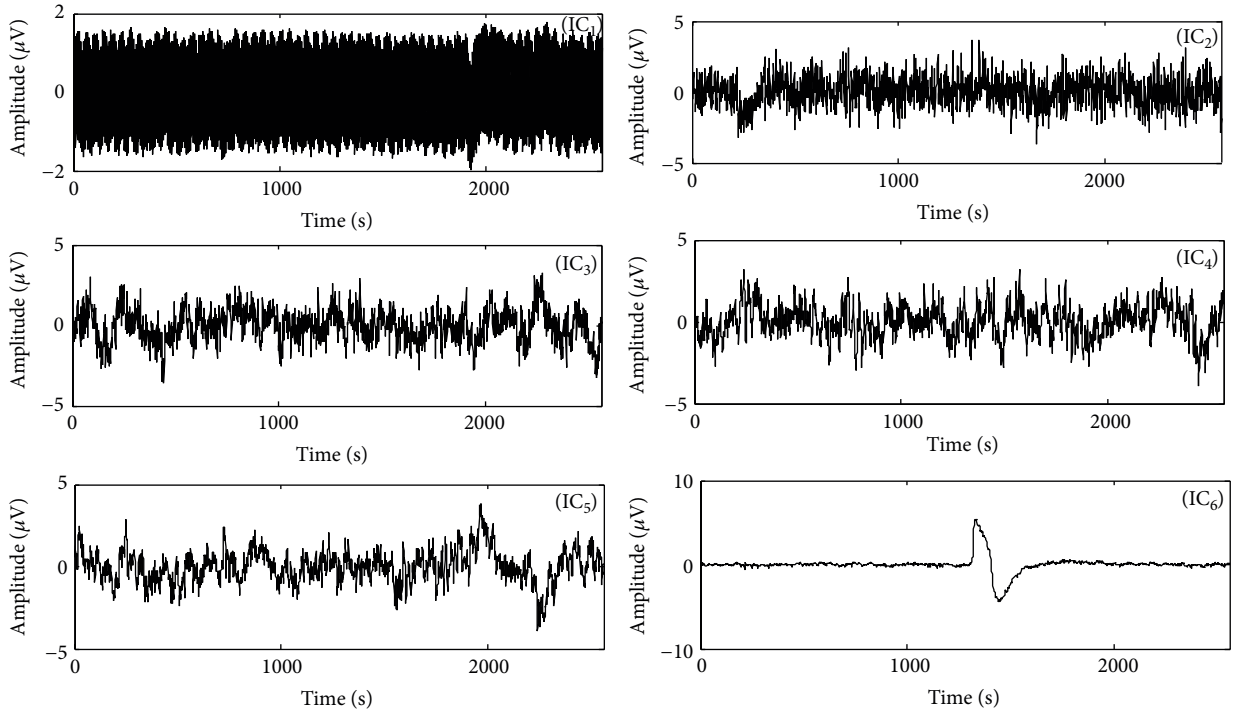

Figure 28: Separated components for Data set I by ESBSS.

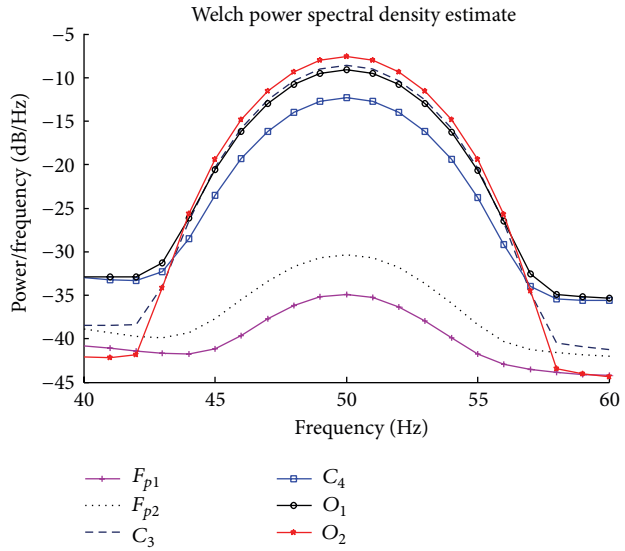

Figure 29: Frequency components of the recorded EEG channels (Data set I) around 50 Hz frequency.

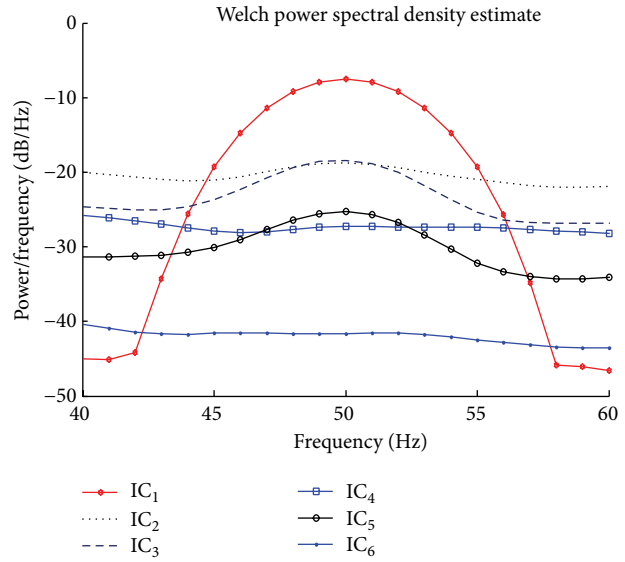

Figure 30: Frequency components of the extracted components for Data set I around 50 Hz frequency.

Table 18: Types of separated signals from data set I of the proposed algorithm using sparsity measure.

IC	Sparsity	Type of IC
IC$_1$	0.1641	**Line noise**
IC$_2$	1.5678	Brain signal
IC$_3$	1.4921	Brain signal
IC$_4$	1.7374	Brain signal
IC$_5$	1.9785	Brain signal
IC$_6$	11.5523	**Artifact**

6. Conclusion

Automatic artifact extraction system is proposed based on evolutionary Stone's BSS algorithm ESBSS. The system has been proven to be a powerful technique for extracting both super-Gaussian signal and sub-Gaussian signal from brain EEG mixtures automatically and simultaneously. ESBSS was shown to perform better than different types of blind source separation algorithms as demonstrated in simulated and experimental results. The proposed system solves many problems by the hybridization process between the original BSS and genetic algorithm. Almost the previous works in the artifact extraction field used notch filter as a preprocessing step to remove power line noise but, in the proposed

Table 19: Correlation measure between EOG channels and the extracted artifacts for different BSS.

BSS algorithms	Correlation between vEOG and estimated eye blink artifact	Correlation between hEOG and estimated eye muscle artifact
EBSS	0.9953	0.9899
EFICA	0.9844	0.9811
Stone	0.9759	0.9801
FICA	0.9713	0.9759
SOBI	0.9704	0.9788
BGSEP	0.9901	0.9789
JADE	0.9622	0.9721

Table 20: Types of separated signals from data set II of the proposed algorithm using sparsity measure.

Components	Sparsity	Type of IC
IC_1	0.1521	**Line noise**
IC_2	1.4997	Brain signal
IC_3	1.2434	Brain signal
IC_4	1.7249	Brain signal
IC_5	4.9024	**Artifact**
IC_6	5.4787	**Artifact**

Table 21: Performance measure based on cross-correlation measurement.

BSS methods	Correlation between vEOG and estimated eye blink (IC_1)
EBSS	0.9956
EFICA	0.9511
Stone	0.9134
FICA	0.8926
SOBI	0.8819
JADE	0.8001

Table 22: Types of separated signals from real EEG data (19 channels) of the proposed algorithm using sparsity measure.

IC	Sparsity	Type of IC
IC_1	11.476	**Artifact**
IC_2	2.0036	Brain signal
IC_3	2.1521	Brain signal
IC_4	1.9057	Brain signal
IC_5	2.1731	Brain signal
IC_6	1.9003	Brain signal
IC_7	0.2426	**LN**
IC_8	2.1129	Brain signal
IC_9	1.3741	Brain signal
IC_{10}	2.2244	Brain signal
IC_{11}	1.5671	Brain signal
IC_{12}	1.9621	Brain signal
IC_{13}	1.2986	Brain signal
IC_{14}	1.0013	Brain signal
IC_{15}	1.1021	Brain signal
IC_{16}	1.0318	Brain signal
IC_{17}	1.0119	Brain signal
IC_{18}	1.0093	Brain signal
IC_{19}	1.0014	Brain signal

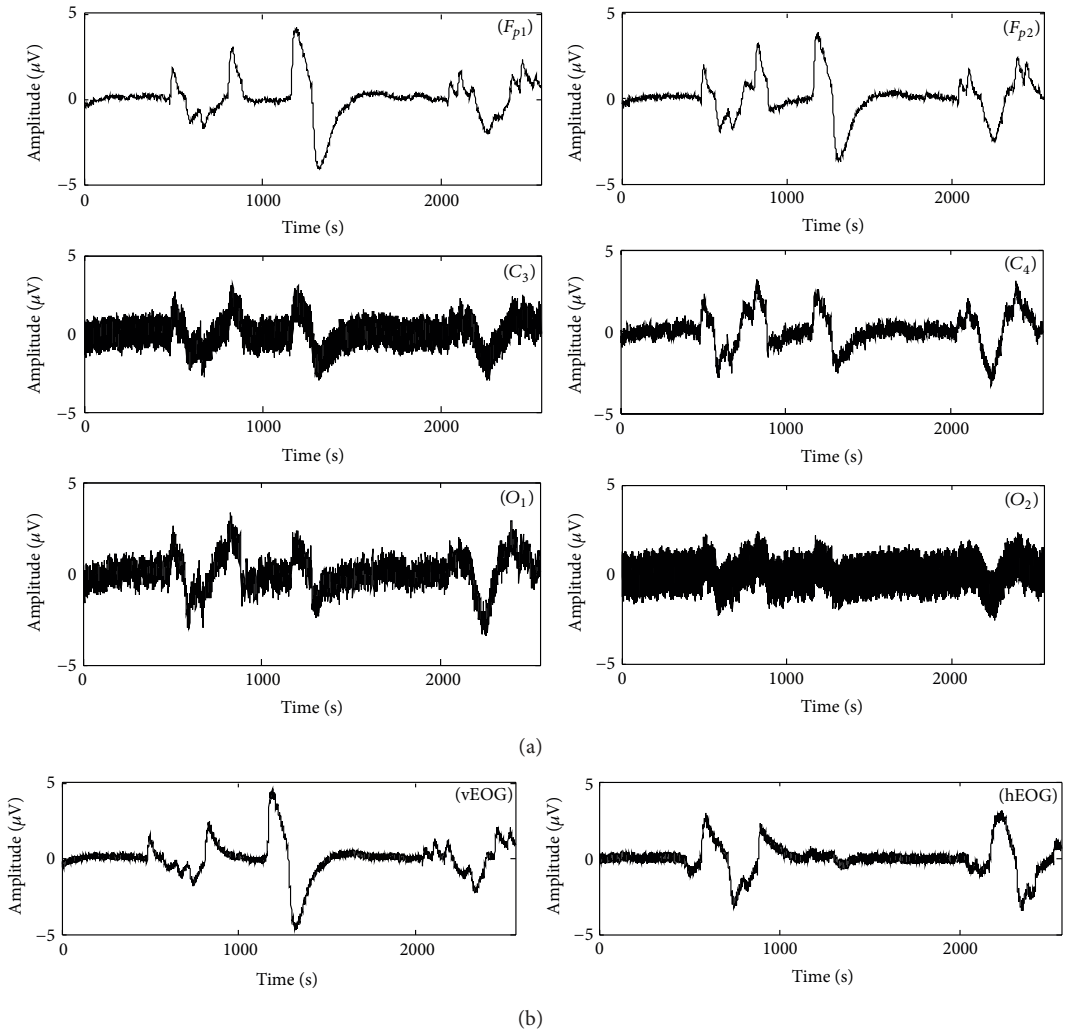

Figure 31: Data set II with zero mean and unit variance: (a) EEG electrodes; (b) EOG electrodes.

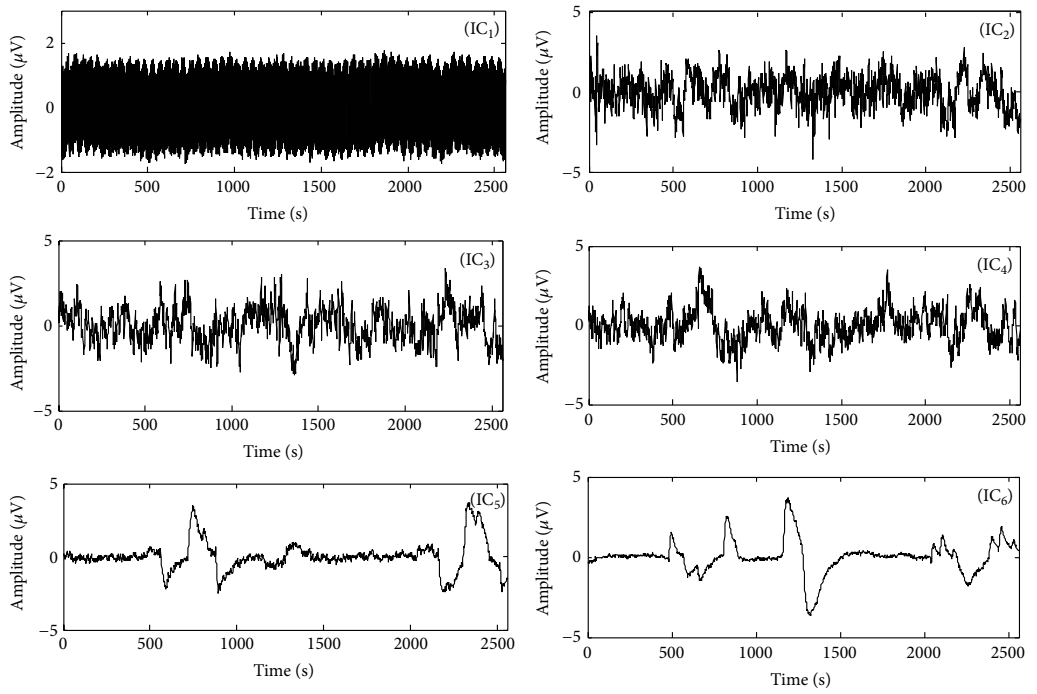

Figure 32: Separated components by ESBSS.

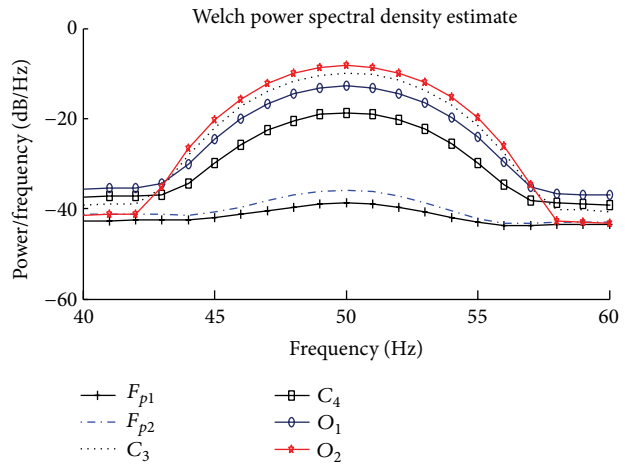

Figure 33: Frequency components of the recorded EEG channels (Data set II) around 50 Hz frequency.

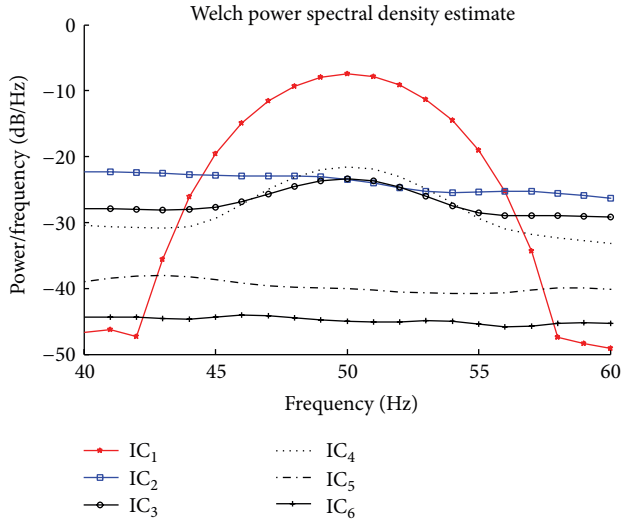

Figure 34: Frequency components of the extracted components for Data set II around 50 Hz frequency.

Figure 35: Computerized EEG system (Ibn-Rushd Hospital, Baghdad, Iraq).

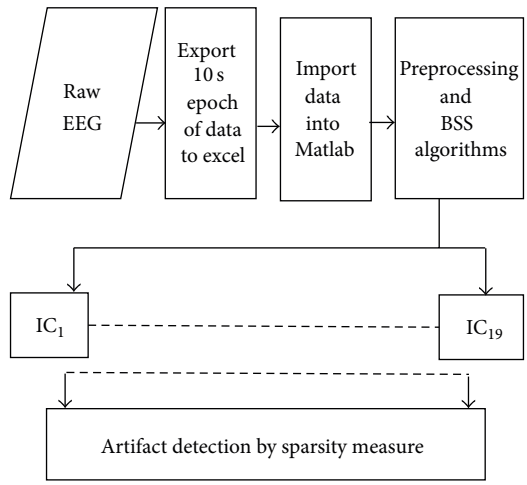

Figure 36: Flowchart of the overall system process.

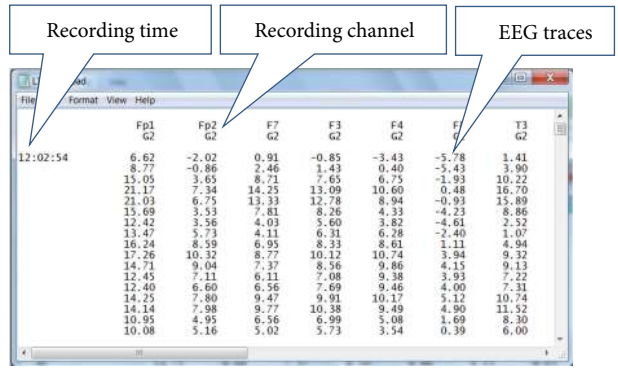

Figure 37: An ASCII file opens in a Notepad program.

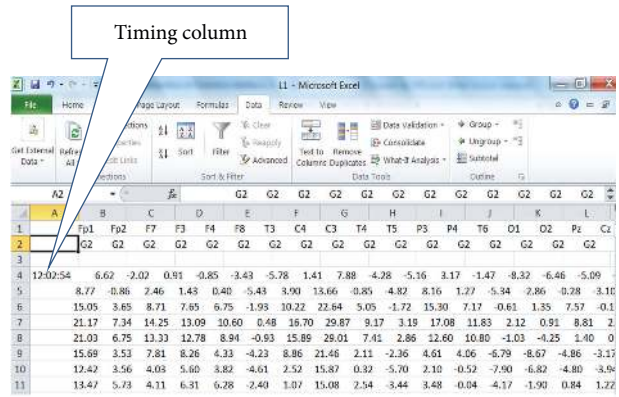

Figure 38: The Excel window that contains the EEG trace.

system, there is no filter used in order not to lose any information. The results obtained by the ESBSS algorithm are encouraging and can be used to extract other types of artifacts.

Conflict of Interests

The authors declare that there is no conflict of interests regarding the publication of this paper.

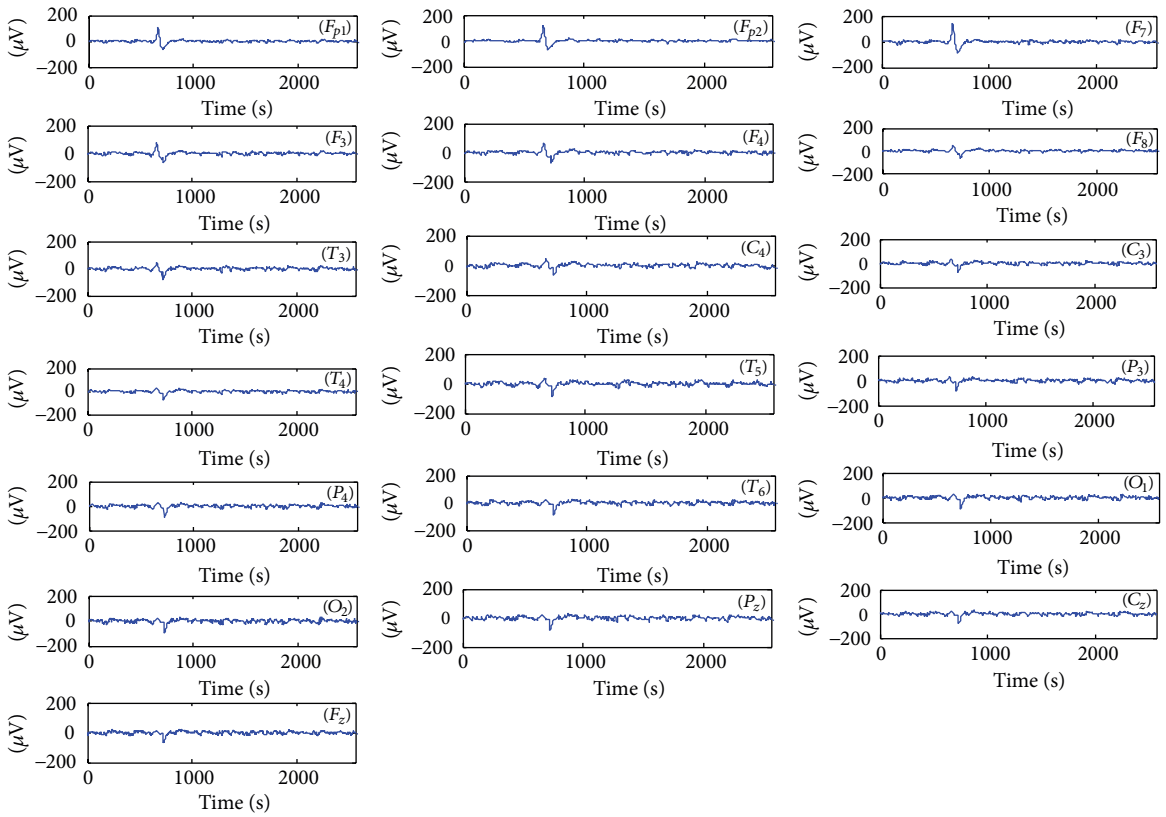

FIGURE 39: Signals measured by a computerized EEG device, x-axis represent signal amplitude in microvolt and y-axis represent time in second.

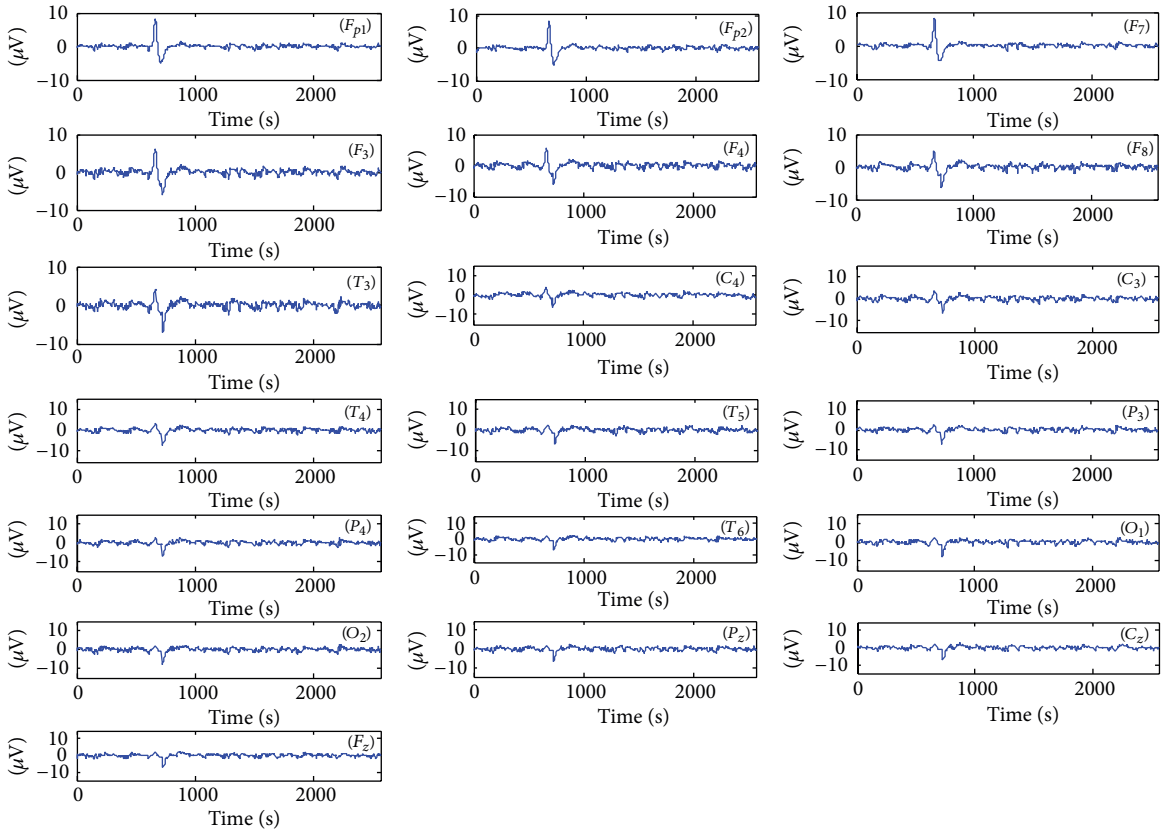

FIGURE 40: Measured signals with unite mean and unite variance, x-axis represent signal amplitude in microvolt and y-axis represent time in second.

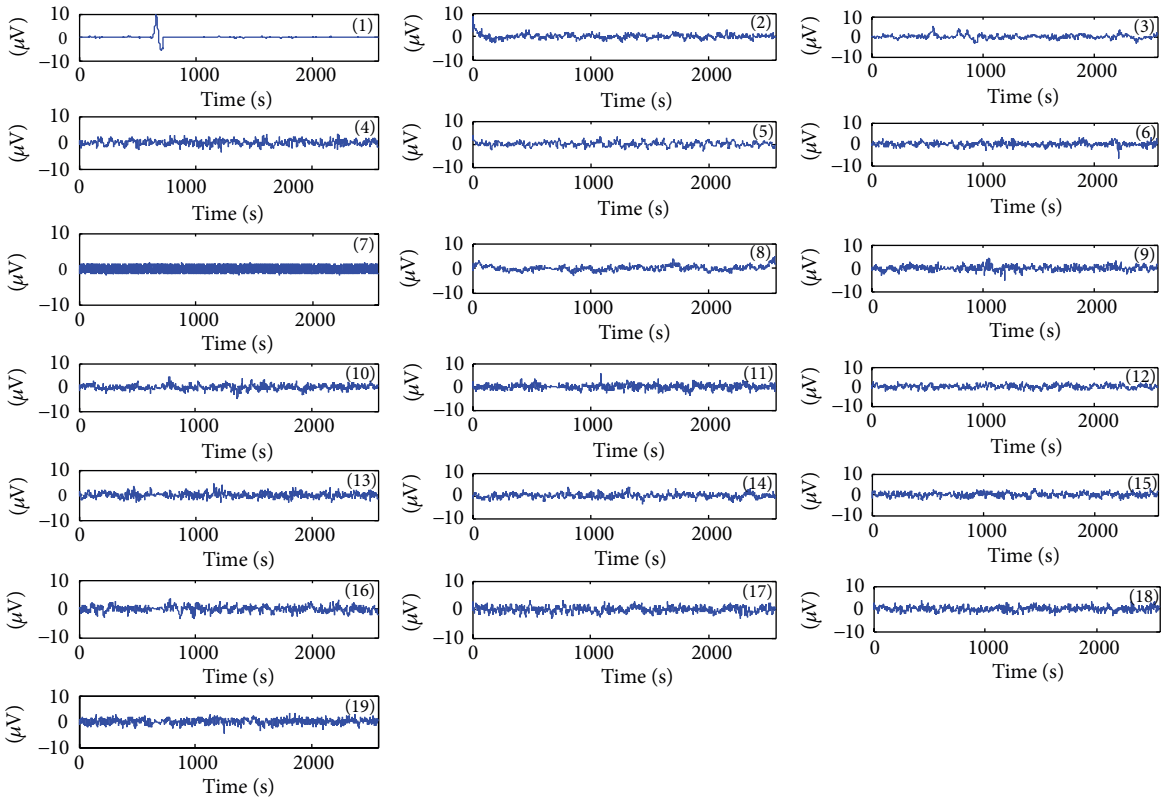

Figure 41: Separated signals by ESBSS algorithm.

Acknowledgments

This work was supported by the National Natural Science Foundation of China (Grant no. 61172159) and the Fundamental Research Funds for the Central Universities (HEUCFT1101). The authors would like to express their thanks to Dr. Danilo P. Mandic, Imperial College, United Kingdom, for giving them real data (8 channels data); also they express their thanks to Mr. Salim, Wasit University, Iraq, for giving them real data (19 channels).

References

[1] M. Zima, P. Tichavsk, K. Paul, and V. Krajča, "Robust removal of short-duration artifacts in long neonatal EEG recordings using wavelet-enhanced ICA and adaptive combining of tentative reconstructions," *Physiological Measurement*, vol. 33, no. 8, pp. N39–N49, 2012.

[2] T. Rasheed, *Constrained blind source separation of human brain signals [Ph.D. thesis]*, Department of Computer Engineering, Kyung Hee University, Seoul, Republic of Korea, 2010.

[3] M. A. G. Correa and E. L. Leber, "Noise removal from EEG signals in polisomnographic records applying adaptive filters in cascade," in *Adaptive Filtering Applications*, L. Garcia, Ed., 2011.

[4] A. Delorme, T. Sejnowski, and S. Makeig, "Enhanced detection of artifacts in EEG data using higher-order statistics and independent component analysis," *NeuroImage*, vol. 34, no. 4, pp. 1443–1449, 2007.

[5] M. T. Akhtar, C. J. James, and W. Mitsuhashi, "Modifying the spatially-constrained ICA for efficient removal of artifacts from EEG data," in *Proceedings of the 4th International Conference on Bioinformatics and Biomedical Engineering (iCBBE '10)*, pp. 1–4, Chengdu, China, June 2010.

[6] C. A. Joyce, I. F. Gorodnitsky, and M. Kutas, "Automatic removal of eye movement and blink artifacts from EEG data using blind component separation," *Psychophysiology*, vol. 41, no. 2, pp. 313–325, 2004.

[7] Z. Xue, J. Li, S. Li, and B. Wan, "Using ICA to remove eye blink and power line artifacts in EEG," in *Proceedings of the 1st International Conference on Innovative Computing, Information and Control*, Beijing, China, August 2006.

[8] A. Cichocki and S. Amari, *Adaptive Blind Signal and Image Processing: Learning Algorithms and Applications*, John Wiley & Sons, New York, NY, USA, 2005.

[9] C. W. De, A. Vergult, B. Vanrumste et al., "A new muscle artifact removal technique to improve the interpretation of the ictal scalp electroencephalogram," in *Proceedings of the 27th Annual International Conference of the Engineering in Medicine and Biology Society (IEEE-EMBS '05)*, pp. 944–947, Shanghai, China, September 2005.

[10] H. Ghandeharion and H. Ahmadi-Noubari, "Detection and removal of ocular artifacts using independent component analysis and wavelets," in *Proceedings of the 4th International IEEE/EMBS Conference on Neural Engineering (NER '09)*, pp. 653–656, Antalya, Turkey, May 2009.

[11] J. Pesin, *Detection and removal of eyeblink artifacts from EEG using wavelet analysis and independent component analysis, [Msc thesis]*, Department of Electrical Engineering, Rochester

Institute of Technology; Kate Gleason College of Engineering, New York, NY, USA, 2007.

[12] A. J. Bell and T. J. Sejnowski, "An information-maximization approach to blind separation and blind deconvolution.," *Neural computation*, vol. 7, no. 6, pp. 1129–1159, 1995.

[13] A. Hyvärinen and E. Oja, "A Fast fixed-point algorithm for independent component analysis," *Neural Computation*, vol. 9, no. 7, pp. 1483–1492, 1997.

[14] A. Belouchrani, K. Abed-Meraim, J. Cardoso, and E. Moulines, "A blind source separation technique using second-order statistics," *IEEE Transactions on Signal Processing*, vol. 45, no. 2, pp. 434–444, 1997.

[15] D. Pham and J. Cardoso, "Blind separation of instantaneous mixtures of nonstationary sources," *IEEE Transactions on Signal Processing*, vol. 49, no. 9, pp. 1837–1848, 2001.

[16] P. Tichavský and Z. Koldovský, "Fast and accurate methods of independent component analysis: a survey," *Kybernetika*, vol. 47, no. 3, pp. 426–438, 2011.

[17] A. Ahmed, Z. C. Zhu, and C. Yan, "A novel evolutionary approach for blind source separation based on stone's method," in *Proceedings of the 11th International Conference on Signal Processing (ICSP '12)*, pp. 324–328, Beijing, China, October 2012.

[18] A. K. Abdullah and Z. C. Zhu, "Blind source separation techniques based of brain computer interface system: a review," *Research Journal of Applied Sciences, Engineering and Technology*, vol. 7, pp. 484–494, 2014.

[19] A. K. Abdullah, Z. C. Zhu, L. Siyao, and S. M. Hussein, "Blind source separation techniques based eye blinks rejection in EEG signals," *Information Technology Journal*, vol. 13, pp. 401–413, 2014.

[20] J. V. Stone, "Blind source separation using temporal predictability," *Neural Computation*, vol. 13, no. 7, pp. 1559–1574, 2001.

[21] J. V. Stone, "Blind deconvolution using temporal predictability," *Neurocomputing*, vol. 49, pp. 79–86, 2002.

[22] M. Ye and X. Li, "An efficient measure of signal temporal predictability for blind source separation," *Neural Processing Letters*, vol. 26, no. 1, pp. 57–68, 2007.

[23] M. Khosravy, M. R. Asharif, and K. Yamashita, "A theoretical discussion on the foundation of Stone's blind source separation," *Signal, Image and Video Processing*, vol. 5, no. 3, pp. 379–388, 2011.

[24] L. F. Nicolas-Alonso and J. Gomez-Gil, "Brain computer interfaces, a review," *Sensors*, vol. 12, no. 2, pp. 1211–1279, 2012.

[25] H. H. Jasper, "The ten twenty electrode system of the International Federation," *Electroencephalography and Clinical Neurophysiology*, vol. 10, pp. 371–375, 1958.

[26] B. J. Fisch and R. Spehlmann, *Fisch and Spehlmann's EEG Primer: Basic Principles of Digital and Analog EEG*, Elsevier, 3rd edition, 1999.

[27] S. M. Hussein, *Design and implementation of AI controller based on brain computer interface [Master, thesis]*, Computer Engineering, Nahrain University, Baghdad, Iraq, 2007.

[28] S. Sanei and J. A. Chambers, *EEG Signal Processing*, John Wiley & Sons, England, UK, 1st edition, 2007.

[29] L. Sörnmo and P. Laguna, *Bioelectrical Signal Processing in Cardiac and Neurological Applications*, Elseiver, New York, NY, USA, 1st edition, 2005.

[30] J. N. Knight, *Signal fraction analysis and artifact removal in EEG [M.S. thesis]*, Computer Science, Colorado State University, Boulder, Colo, USA, 2003.

[31] L. Vigon, M. R. Saatchi, J. E. W. Mayhew, and R. Fernandes, "Quantitative evaluation of techniques for ocular artefact filtering of EEG waveforms," *IEE Proceedings: Science, Measurement and Technology*, vol. 147, no. 5, pp. 219–228, 2000.

[32] A. Crespel, P. Gélisse, M. Bureau, and P. V. Genton, *Atlas of Electroencephalography*, vol. 1, J. Libbey Eurotext, Paris, France, 1st edition, 2005.

[33] T. Jung, S. Makeig, C. Humphries et al., "Removing electroencephalographic artifacts by blind source separation," *Psychophysiology*, vol. 37, no. 2, pp. 163–178, 2000.

[34] S. V. Ramanan, N. V. Kalpakam, and J. S. Sahambi, "A novel wavelet based technique for detection and de-noising of ocular artifact in normal and epileptic electroencephalogram," in *Proceedings of the International Conference on Communications, Circuits and Systems*, vol. 2, pp. 1027–1031, June 2004.

[35] G. L. Wallstrom, R. E. Kass, A. Miller, J. F. Cohn, and N. A. Fox, "Automatic correction of ocular artifacts in the EEG: a comparison of regression-based and component-based methods," *International Journal of Psychophysiology*, vol. 53, no. 2, pp. 105–119, 2004.

[36] T. W. Picton, P. Van Roon, M. L. Armilio, P. Berg, N. Ille, and M. Scherg, "The correction of ocular artifacts: a topographic perspective," *Clinical Neurophysiology*, vol. 111, no. 1, pp. 53–65, 2000.

[37] J. Lehtonen, *EEG-based brain computer interfaces [M.S. thesis]*, Electrical and communication Engineering Department, University of Technology, Helsinki, Finland, 2002.

[38] S. Mavaddaty and A. Ebrahimzadeh, "Blind signals separation with genetic algorithm and particle swarm optimization based on mutual information," *Radioelectronics and Communications Systems*, vol. 54, no. 6, pp. 315–324, 2011.

[39] A. Hyvarinen, J. Karhunen, and E. Oja, *Independent Component Analysis*, John Wiley & Sons, New York, NY, USA, 2001.

[40] F. Rojas, C. G. Puntonet, M. R. Álvarez, and I. Rojas, "Evolutionary algorithm using mutual information for independent component analysis," in *Proceedings of the 7th International Work-Conference on Artificial and Natural Neural Networks (IWANN '03)*, pp. 233–240, Menorca, Spain, June 2003.

[41] S. Kai, W. Qi, and D. Mingli, "Approach to nonlinear blind source separation based on niche genetic algorithm," in *Proceedings of the 6th International Conference on Intelligent Systems Design and Applications (ISDA '06)*, pp. 441–445, Jinan, China, October 2006.

[42] J. V. Stone, *Independent Component Analysis: A Tutorial Introduction*, A Bradford Book, London, UK, 2004.

[43] Z. Koldovský, P. Tichavský, and E. Oja, "Efficient variant of algorithm FastICA for independent component analysis attaining the Cramér-Rao lower bound," *IEEE Transactions on Neural Networks*, vol. 17, no. 5, pp. 1265–1277, 2006.

[44] V. Mäkinen, H. Tiitinen, and P. May, "Auditory event-related responses are generated independently of ongoing brain activity," *NeuroImage*, vol. 24, no. 4, pp. 961–968, 2005.

[45] L. Shoker, S. Sanei, and M. A. Latif, "Removal of eye blinking artifacts from eeg incorporating a new constrained bss algorithm," in *Proceeding of the 26th Annual International Conference of the IEEE Engineering in Medicine and Biology Society (EMBC '04)*, pp. 909–912, San Francisco, Calif, USA, September 2004.

[46] S. Xian-Bin, P. Shao-Jin, and S. Mei-Qin, "The EEG processing algorithm based on improved ICA," in *Proceedings of the 15th International Conference on Digital Image Processing (ICDIP '13)*, 2013.

[47] B. M. Abadi, D. Jarchi, and S. Sanei, "Simultaneous localization and separation of biomedical signals by tensor factorization," in *Proceedings of the IEEE/SP 15th Workshop on Statistical Signal Processing (SSP '09)*, pp. 497–500, Cardiff, UK, September 2009.

[48] S. Javidi, D. P. Mandic, C. C. Took, and A. Cichocki, "Kurtosis-based blind source extraction of complex non-circular signals with application in EEG artifact removal in real-time," *Frontiers in Neuroscience*, vol. 5, p. 105, 2011.